KINETIC MODEL OF PERFLUOROALKYL SUBSTANCES REMOVAL FROM ENVIRONMENTAL MATRICES VIA ELECTRON BEAM IRRADIATION

A Thesis

by

RUILIAN GAO

Submitted to the Office of Graduate and Professional Studies of
Texas A&M University
in partial fulfillment of the requirements for the degree of

MASTER OF SCIENCE

Chair of Committee,	David Staack
Committee Members,	Suresh D. Pillai
	Choongho Yu
Head of Department,	Andreas Polycarpou

December 2020

Major Subject: Mechanical Engineering

ABSTRACT

Per- and polyfluorylalkyl substances (PFASs) products, including perfluorooctanoic acid (PFOA) and perfluorooctane sulfonate (PFOS), were widely produced in the industry and commercial products. They were detected in natural waters and soil matrix. The bond energy of carbon-fluorine in PFASs lead the high difficulty of breakdown. Previous study proved the toxicity and bioaccumulation of PFASs. A cost-effective and efficient way to decompose PFASs in water and soil matrix has to be investigated.

Electron beam with high energy after an accelerator can generate a large number of reactive species in water like hydrated electron (e_{aq}^-), hydroxyl radical ($^{\bullet}OH$), and hydrogen radical ($H^{\bullet}$). These reducing and oxidizing agents play an important role to break down the carbon-fluorine bond based on the previous studies.

10 MeV, 15kW electron beam was used to individually treat PFOA, PFOS, and PFHpA solution at 100 μg/L in HPLC water, groundwater samples from Pennsylvania, soil samples from Michigan. The effect of different pH values, concentrations of bicarbonate, nitrate, and fulvic acid were studied to investigate during PFHpA degradation. Preliminary results show that > 14.61% PFOA removal was observed at pH 13.0 with 75 kGy eBeam, and PFOS has the similar decomposition efficiency at the same experiment conditions. The experiment shows that low dose irradiation could not fully remove PFASs in water. For PFHpA, nitrate ion, bicarbonate, and fulvic acid at pH 13.0

in spiked water sample will not have negative effect on breakdown where the removal percentage is 100%. Higher pH had a positive effect on spiked PFHpA sample.

The irradiation experiments of investigation-derived waste (IDW) samples without any pH adjustment with high doses from 0 to 2000 kGy showed the increasing degradation percentage of PFASs. For Pennsylvania water sample, the breakdown percentage was about 88% at 2000 kGy. For PFOS was rapidly degraded until 1000 kGy, while PFHpA firstly increased before 500 kGy and then breakdown until 2000 kGy.

Further, kinetic model was proposed to investigate the possible pathway of PFAS breakdown. All the concentration or mass of degradation products and PFOA, PFOS satisfied the pseudo first kinetic order. At the PA-WATER field sample, PFOA and PFOS were decomposed with the rate constant of 1.21×10^{-3} $kGy^{-1}s^{-1}$, 3.3×10^{-4} $kGy^{-1}s^{-1}$ respectively. The reaction kinetics of short chain PFAS (PFHpA) was $< 2.16 \times 10^{-3}$ $kGy^{-1}s^{-1}$, almost one order magnitude larger than other short chain PFAS.

This study proves the high efficiency of eBeam as a promising technology that can be performed to remediate PFASs and other co-contaminants in aqueous and solid environmental matrices such as groundwater and soils.

CONTRIBUTORS AND FUNDING SOURCES

Contributors

This work was done with much help of Professor David Staack, Professor Suresh Pillai of the Department of Nutrition and Food Science and Professor Choongho Yu from Mechanical Engineering Department.

Spike water and soil samples were prepared with the help of Corinne Kowald from the Department of Nutrition and Food Science.

High-dose trials were done with help from my lab mates such as John Lassalle and Bob Rodi. Solid-phase extraction and spiked PFHpA are done with the help of Postdoc Mingbao Feng from the School of Public Health.

Concentration analysis by LC-MS was performed by the Integrated Metabolomics Analysis Core (IMAC) at Texas A&M University and SGS-AXYS in British Colombia, Canada.

All other work conducted for the thesis was completed by the student independently.

Funding Sources

This work was funded from Chevron U.S.A. Inc. 0015096913-M1803767, SERDP-ESTCP project ER 18-1620, and EPA project G2018-STAR-B1. Its contents are solely the responsibility of the authors and do not necessarily represent the official views of the DOE, EPA, and Chevron.

NOMENCLATURE

AFFFs:	Aqueous Fire Fighting Foams
°C	Degree Celsius
EPA	U.S. Environmental Protection Agency
GAC	Granular Activated Carbon
HPLC	High-Performance Liquid Chromatography
HDPE	High-Density Polyethylene
IDW	Investigation Derived Waste
IMAC	Integrated Metabolomics Analysis Core
kGy	Kilogray
LC-MS	Liquid Chromatography-Mass Spectrometry
LINAC	Linear Accelerator
MeV	Mega Electron Volts
PFASs	Per- and Polyfluoroalkyl Substances
PFBA	Perfluorobutyric acid
PFBS	Perfluorobutanesulfonic acid
PFOA	Perfluorooctanoic acid
PFOS	Perfluorooctanesulfonic acid
PFOS-K	Potassium salt of PFOS
PFHpA	Perfluoroheptanoic acid
PFHpS	Perfluoroheptanesulfonic acid

PFHxA	Perfluorohexanoic acid
PFHxS	Perfluorohexanesulfonic acid
PFHeA	Perfluoropentanoic acid
PFHeS	Perfluoropentanesulfonic acid
ppt	Parts Per Trillion
ppm	Parts Per Million
PPE	Personal Protective Equipment
PTFE	Polytetrafluoroethylene
SPE	Solid-Phase Extraction
UV	Ultraviolet
VUV	Vacuum Ultraviolet

TABLE OF CONTENTS

LIST OF FIGURES

Page

LIST OF TABLES

Page

CHAPTER I

INTRODUCTION

1.1 Background

Perfluorinated compounds (PFCs) refer to the strained or branched-chain hydrocarbons, all hydrogen are replaced by fluorine atoms. Since 1938, polytetrafluoroethylene (PTFE) was first discovered by Dr. Plunket from Dupont, per- and polyfluorylalkyl substances (PFASs) products especially perfluorooctanoic acid (PFOA) have been produced as common material.[1] [2] These compounds have high chemical, biological and thermal stability due to the carbon-fluorine bond (116 kcal/mol), thus not easily breakdown by hydrolysis, photolysis, microorganisms, and other traditional methods.[3] PFCs have good thermal stability, hydrophobicity, oleophobicity, and high surface activity, however, bioaccumulation has been proved along with the food chains, among which perfluorooctane sulfonate (PFOS) displayed the highest concentration value.[4]

Among all the PFCs, PFOS and PFOA are two major examples in the aquatic environment. [5] Recent research shows that PFASs have already been in the water cycle included drinking water, wastewater, lake water, and groundwater.[6] The advisory concentration of PFOS/PFOA in drinking water is at 70 parts per trillion (ppt) from the regulation of the U.S. Environmental Protection Agency (EPA). It has been demonstrated that the biological method could lead to C-C bond's breakdown rather than C-F.[7] Traditional wastewater treatments like adsorption by granular activated carbon (GAC) are

limited by size, efficiency and load compacity.[8] Therefore, long-chain PFAS breakdown needs more investigation, and a more cost-efficient way should be found.

1.2 Thesis Statement

This thesis describes the application of a high energy electron beam (eBeam) on the removal of PFASs in wastewater and soil. The Chapter II introduces the major chemical properties and toxicity of PFASs, especially PFOA and PFOS. Existing methods for PFAS remediation are compared in detail. Based on some basic theories about the production of the electron beam and dose measurement are also discussed. The Chapter III describes the experimental design, and analytical procedures, and the modeling method. The Chapter IV presents the results of PFAS decomposition by electron beam and propose a model via analyzing the experimental and modeling results.

1.3 Motivation

Since PFASs are found in our drinking water and used in many commercial products. These kinds of chemicals are hazardous, which could increase the risk of cancer, thyroid and liver disorders, high cholesterol, weakened immune system, and so on.[9] So, EPA set a health advisory at 70 ppt. U.S. military and NATO used Aqueous firefighting foams (AFFF) as firefighting foams containing PFOS since 1960s.[10]

Electron beam technology generates the hydrated electron (e_{aq}^-), hydrogen radical (H•), and hydroxyl radical (•OH) during the irradiation of water. The full range of PFASs with different amounts of carbon atoms could be broken down.

1.4 Hypothesis

1. eBeam technology is comparably effective on short and long change PFAS removal.
2. Some additives (nitrate ion, bicarbonate, and fulvic acid) can inhibit PFAS breakdown in water.
3. Higher pH values could sharply increase the PFAS decomposition efficiency.
4. Kinetic studies can be used to help see what the important factors (pH, additives) for degradation efficiency of PFAS.

1.5 Objectives

1. Explore the use of low-dose eBeam for removing PFOA/PFOS/PFHpA in water by optimizing the experimental parameters, e.g., additives, pH, and oxygen content.
2. Characterize and quantify the effectiveness of high dose eBeam at degrading PFASs in field samples.
3. Developing a kinetic model to describe eBeam remediation of PFOA/POFS contaminated samples.

CHAPTER II

LITERATURE REVIEW

2.1 PFASs

As shown in Figure 1, there has been an increasing number of researches regarding "PFOA", "PFOS", and "PFAS", which could be illustrated by the number of publications from 2010 – 2020 at ISI Web of Science.

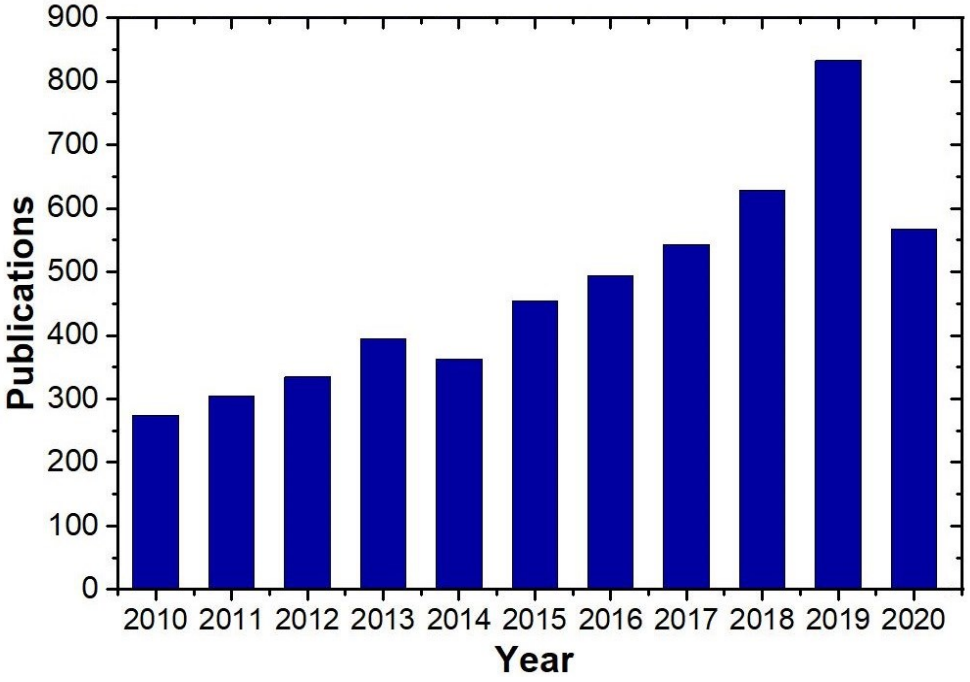

Figure 1: The number of publications from the ISI Web of Science for the keywords of "PFOA" or "PFOS" or "PFAS" (Oct. 2020).

A typical compound of perfluorocarboxylate anions (PFCAs) is perfluorooctanoate ($C_7F_{15}COO$-, PFOA) (Figure 2)[11], and only PFOA and perfluorononanoic acid (PFNA) are chosen to be industrially produced among all PFCAs

(Figure 3).[12] PFOS could not degrade in natural environments or common water treatment methods as the result of C-F bond. [13](Table 1)

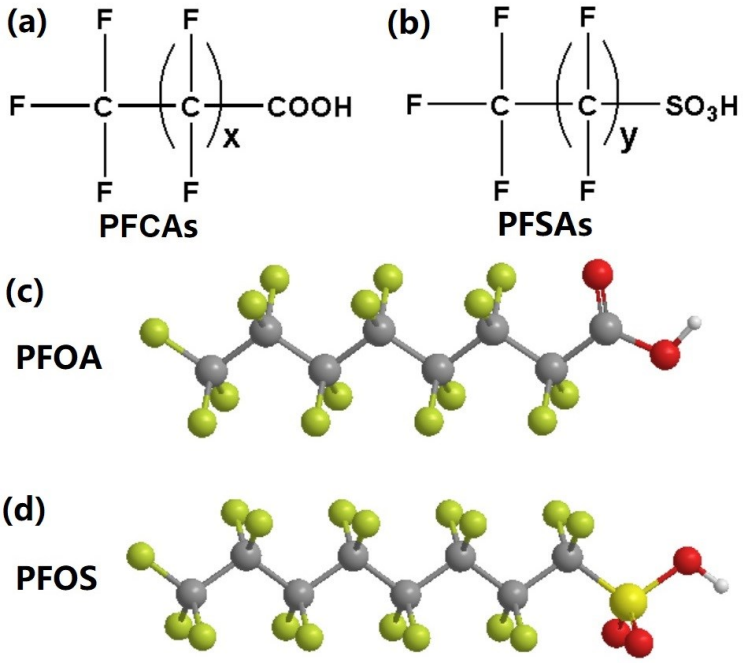

Figure 2: Chemical structure of (a) PFCAs, (b) PFSAs, and two representative compounds (c) PFOA, (d) PFOS.

Table 1: PFAS properties (boiling point and vapor pressure)

Formula	Proposed name	Boiling point(°C) at 760 mmHg	Vapor pressure at 25°C (mm Hg)
$C_8HF_{17}O_3S$	Perfluorooctane sulfonic acid (PFOS)	258–260	0.002
$C_8HF_{15}O_2$	Perfluorooctanoic acid (PFOA)	192	0.525
$C_7HF_{13}O_2$	Perfluoroheptanoic acid (PFHpA)	177	0.13
$C_6HF_{11}O_2$	Perfluorohexanoic acid (PFHxA)	157	1.98

Table 1: Continued

Formula	Proposed name	Boiling point(°C) at 760 mmHg	Vapor pressure at 25°C (mm Hg)
$C_5HF_9O_2$	Perfluoropentanoic acid (PFPeA)	124.4±35.0	7.9±0.4
($C_4HF_7O_2$)	Perfluorobutanoic acid (PFBA)	121.0	6.37
($C_6F_{13}SO_3H$)	Perfluorohexane sulfonic acid (PFHxS)	238.5	0.0046
$C_4F_9SO_3H$	Perfluorobutane sulfonic acid (PFBS)	211.0	0.0268

2.2 Environmental Occurrence and Toxicity of PFASs

2.2.1 Environmental Occurrence

2.2.1.1 Source of PFASs

Since 1938, polytetrafluoroethylene (PTFE) was first discovered by Dr. Plunket from Dupont, polyfluorylalkyl substances (PFASs) became the important chemical material. [1] Besides that, aqueous film-forming foam (AFFF) contains PFASs was widely used as firefighting foam by U.S. Military since 1960s, which led to the soil and groundwater contamination. [14]

PFOS has two different chemical structures: linear and branched.[15] The adsorption of these two different chemical structures of PFAS isomers to soil and sediment is different.[16] The main production of perfluorinated compounds including PFOS and PFOA was from electrochemical fluorination and the byproduct of fluorinated telomers breakdown. Branched chain isomers account for about 30% of all the PFOS by using

electrochemical fluorination method. (Figure 3) [17] Among that, linear isomers were produced by DuPont (Wilmington, DE) and other companies with telomerization method. [18] Most of the PFOS nowadays in environment were linear isomers. Telomerization technology was applied to many commercial products such as coating for paper packing, semiconductor manufacture.(Figure 3)

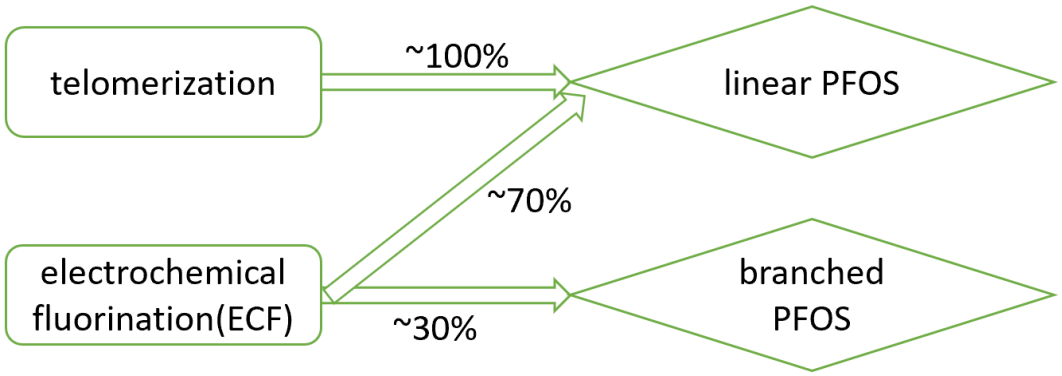

Figure 3: Source of linear PFOS and branched isomers

2.2.1.2 PFASs in Water

The main source of PFASs in water is the direct discharge of fluorine-containing wastewater from industrial production or the disposal from incomplete wastewater treatment. A study of Sharma et al. observed that 15 PFAS were detected in the groundwater and along with Ganges River with 4.7 ng/L PFHxA and 10.2 ng/L PFBS. [19] Lu et al. investigated the total amount of PFASs in Shanghai, China was at most up to 212 ng/L, and PFOA, PFHxA and PFBS were the most common PFASs.[20]

In the USA, the worst PFAS pollution of drinking water was in the middle of Ohio Valley. Water districts near DuPont chemical factory were detected PFOA. [21] The investigation results show that mean concentration of PFAS is 200 ng/L in drinking water. [22] More than 20 states including Texas, Pennsylvania, Michigan, and Oklahoma had

reported the presence of PFASs. [23] The third Unregulated Contaminant Monitoring Rule (UCMR 3) was developed by EPA to regulate analytical methods for monitoring 30 contaminants containing PFASs (Figure 4). Crone et al. study showed reported that high concentration of PFBS in water with 212 ng/L, and PFOS with 7,000 ng/L. [24]

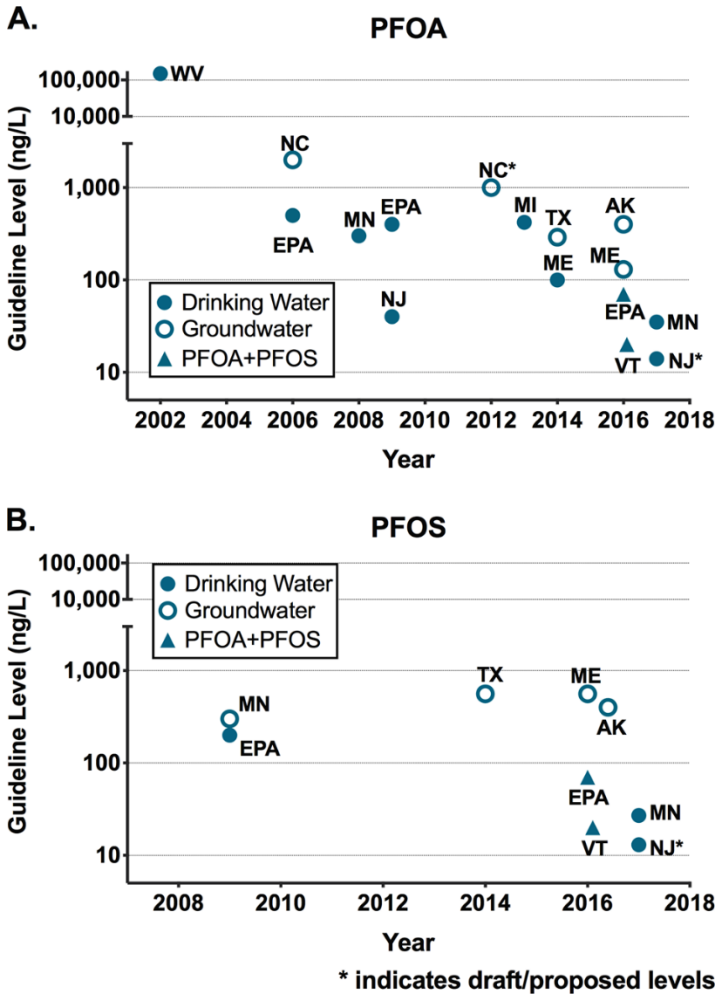

Figure 4: Different required concentration of PFOA/PFOS in drinking water. Reprinted with permission from [25]

2.2.1.3 PFASs in Soil

As an important part of natural waters, soil and bottom mud have become important matrix for hydrophobic organic pollutants. The adsorption and desorption in the soil affect their migration to the environment through groundwater flow. Soil is an important reservoir for PFASs.[26]

The removal of PFASs in soil matrix is extremely hard. Xiao et.al investigated the concentration of PFOA/PFOS in soil, the highest level is 125.7 ng/g, and concentration increased with deeper soil.[27] It was found that PFOS in AFFF was kept during snow melting in soil.[28] One study indicated that the amount of PFOA in soil were related with organic content.[29]

From PFAS contaminated soil survey[30], total PFAS concentrations sampled in all areas upper to 237 μg/kg. The median maximum concentration was 2.7 μg/kg for PFOS/PFOA. Figure 5 shows that PFOS concentrations in surface soil is larger than in deeper soil.

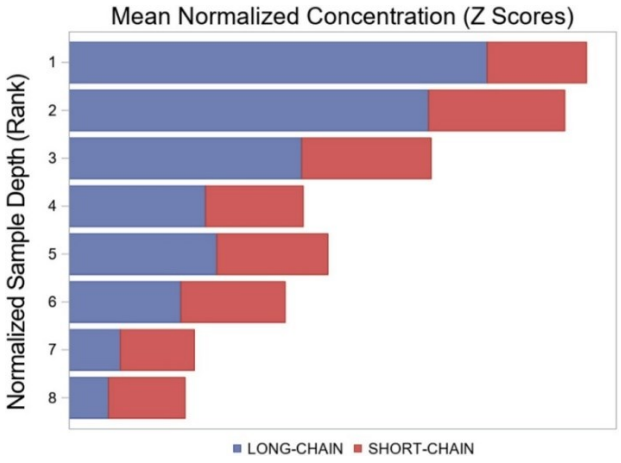

Figure 5: Depth distribution of PFASs in soil matrix. Reprinted with permission from [30]

2.2.2 Toxicity of PFASs

Many studies investigated the toxicity and bioaccumulation of PFASs for human and animal health. PFOS and PFOA persist in human body with several years as a result of stable chemical property. [31] PFOA could exist in the blood and liver of the organism for a long time, so it will cause serious damage to the nervous system, immune system, and reproductive system.[32] The most prevalent and most studied health effects from PFAS ingestion in humans are: thyroid disruption, high blood pressure, birth defects, and suspected carcinogenicity.[32]

2.3 Removal Methods of PFASs

Despite the freshwater ecosystem has a limited self-purification capability related to the amounts and kinds of microorganisms [33], PFASs detected in wastewater, groundwater, and lake water exist as the dominant environment contaminants due to their stability. [34] PFASs are difficult to be decomposed by biological treatment, oxidation, and physicochemical process at ambient temperature. [35] At present, the research on the degradation and remediation of perfluorinated compounds is still developing, and the degradation technology is mainly limited to the lab-scale. Recently, most of the researchers working in this topic are focusing on physical treatments like GAC adsorption, advanced oxidation processes (AOPs), biological treatments, and advanced reduction processes (ARPs). [36]

2.3.1 Physical Treatments

2.3.1.1 GAC

Recently, the most common physical treatment for PFAS-polluted water remediation is GAC because of its high removal efficiency at a low cost. [37] Since 2005, PFASs removal efficiency achieved 99% in sewage by GAC from the 3M company. [38] However, PFASs were only adsorbed to GAC rather than fully destroyed.[39] Inyang found that the relatively good removal efficiency was achieved as more than 85% for long-chain PFASs such as PFOS, but a not high result for the short-chain ones.[40]

Adsorption kinetics are investigated from the relationship of adsorbents and adsorbates. Reddy et al. [41] proposed three commonly used kinetic models to explain the relationship between PFAS and GAC like the pseudo-first-order kinetic model. GAC requires 48-240 hours to get the removal limit, among the full-scale of PFAS, PFOS takes much more time than others because of the C – F bond. [42]

The study of adsorption mechanisms is mostly based on the factors affecting the adsorption efficiency, however, only one mechanism cannot be enough due to the complexity of carbon surface chemistry.[43] Hydrophobic effect, diffusion, and electrostatic interaction could be used to explain this process. At Yang's study, the intra-particle diffusion model assuming that is the only rate control.[44] It was observed that compared with long-chain compounds, short-chain PFASs are more suitable for the intra-particle diffusion kinetics model.[45] Chen proposed that there's linear relationship of PFOS adsorption concentration and diffusion.[46]

2.3.1.2 Ion-exchange Resin

Ion exchange resins (IXs) have attracted widespread attention due to its excellent adsorption of short-chain PFASs.[47] PFAS could be removed from water by ion exchange resins due to PFAS chemical structure. The removal efficiency of anion exchange resin for PFASs (99%) is higher than that of non-ion exchange resin (90%) in the natural water environment. [48] Micelle macromolecules are formed inside the adsorbent, which hinders the diffusion of adsorbate particles and reduces the adsorption capacity of the adsorbent on the anion exchange resin. The field wastewater contains a lot of interfering ions, which has a bad influence on adsorption.[40]

2.3.2 Chemical Processes

Persulfate has the oxidation-reduction potential of 2.01 V, which can transfer an electron to free radicals to achieve PFOS degradation. [49] Sulfate radicals are formed because of the breakdown of O-O bond after heating.[50] The reaction rate of sulfate radicals is often lower than 2×10^{-3} s, but it will increase if the temperature gets higher. [51] Zhao's study shows that the reaction rate and oxidation ability of persulfate could be increased by generating a large amount of oxygen free radicals with higher temperatures. [52] Liu and his partners investigated the effect of persulfate on PFOA removal at different temperatures. They analyzed short-chain reaction intermediates like PFHpA, PFPeA, PFBA, and proposed the breakdown mechanisms of loss of CF_2 unit less than PFOA step by step. [53]

$$SO_4^{\cdot-} + C_7F_{15}COOH \rightarrow SO_4^{2-} + HO^{\cdot} + C_7F_{15}COOH^{+\cdot}$$

$$C_7F_{15}COOH^{+\cdot} \rightarrow C_7F_{15}^{\cdot} + CO_2 + H^{+\cdot}$$

$$C_7F_{15}^{\cdot} + HO^{\cdot} \rightarrow C_{16}F_{13}CF_2OH$$

$$C_{16}F_{13}CF_2OH \rightarrow C_{16}F_{13}COF + F^- + H^+$$

$$C_{16}F_{13}COF + H_2O \rightarrow C_{16}F_{13}COO^- + F^- + 2H^+$$

As previously stated, activated persulfate could degrade PFOA efficiently but not for PFOS. [39] A work done by Yang et al. [51] reported that PFOS could be degraded by sulfate radicals.

2.3.3 Advanced Reduction Processes (ARPs)

2.3.3.1 Photochemical Reduction

Photochemical methods to decompose PFASs in water or soil are based on the oxidation process. [54] PFASs do not absorb much light with more than 220 nm wavelength, and the direct photolysis is not enough to break the stable PFOS. [55]Vacuum ultraviolet (VUV) condition could increase the light absorption while PFOA was at the UV range below 280 nm and above 190 nm. After two hours of VUV irradiation, the degradation rate of PFOA reached 67.1%. [56]

Among the UV-based researches, UV/Fe^{3+}, UV/SO_3^{2-} and UV/$S_2O_8^{2-}$ are widely used to degrade PFASs especially PFOA. It was first found in 1927 that chain reaction occurs during photoionization of sulfite. [57] As the equation shows, SO_3^{2-} after UV irradiation will produce the hydrated electrons (e_{aq}^-) under alkaline condition. Bao's experiment illustrated that, after two hours of UV/SO_3^{2-} treatment, the degradation ratio of PFOA reached 26%.[58]

$$SO_3^{2-} + h\nu \rightarrow SO_3^{\cdot -} + e_{aq}^-$$

The UV-activated persulfate oxidation (UV/$S_2O_8^{2-}$) was often used in wastewater treatment. Wang chose 254 nm as the light wavelength together with persulfate. As a similar mechanism with the heated activation process, the O-O bond was broken down with the formation of sulfate radicals. Then hydroxyl radicals are produced by sulfate radicals.[59]

$$S_2O_8{}^{2-} + h\nu \rightarrow 2SO_4^{\cdot -}$$

$$SO_4^{\cdot -} + H_2O \rightarrow SO_4^{2-} + HO^{\cdot} + H^+$$

It was demonstrated that UV/Fe^{3+} could achieve a 97.8% PFOA decomposition rate with the initial concentration is 50μM PFOA after 28 days. [60] Ultraviolet condition increased the Fenton system efficiency by decreasing the time to several hours. In 5 hours, the PFOA removal ratio achieved more than 95% along with the consumption of all H_2O_2.[61] According to the equation, •OH are formed after the reaction between Fe^{3+} and H_2O_2. [61]

$$Fe^{3+} + H_2O_2 \rightarrow Fe^{2+} + HO_2^{\cdot} + H^+$$

Most of the studies were based on the lab-spiked water, this technology could apply on more filed water.

2.3.3.2 Sonochemical Method

Sonochemistry has been widely applied in PFAS degradation because cavitation in aqueous solution, high temperature, low pressure happened at the gas-liquid surface. [62]When determining the sound velocity, 20 – 1000 kHz or more than 0.5 MHz are often been applied. [63] Such high energy input to the water environment results in the formation of many bubbles[64], along with the expansion of bubbles, the temperature

achieved about 5000. The reason for PFAS decomposition is about heat mediated.[65] Lin's study adopted the sonochemical method with the assistant of sulfate and found 99.8% defluorination at the condition of 4.3 pH, 25 °C within 90 min.[66]

2.4 Electron Beam

2.4.1 Electron Beam Generation

As the figure 6 shows, electron beam technology is an cost-effective and quick approach for PFOA/PFOS removal compared with other methods. Electrons are from a thermionic cathode and accelerated toward the anode at the ground potential.

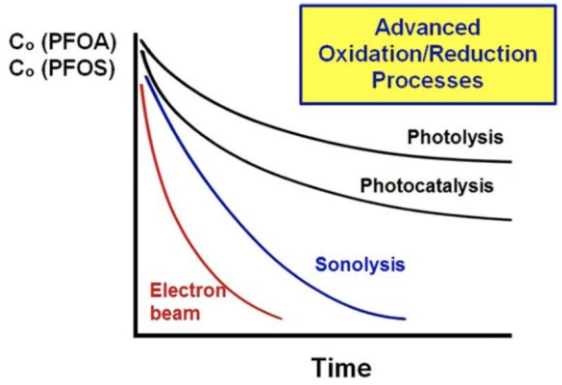

Figure 6: Comparison of different methods of advanced oxidation/reduction process for PFOA and PFOS. Reprinted with permission from [67]

Electrons have enough energy to eject electrons from atoms and molecules. Devices used to transfer energy to electrons are accelerators which are key components of the electron beam irradiation system, All the electrons then suffer additional collisions until all their energy is dissipated by ionization.(Figure 7)

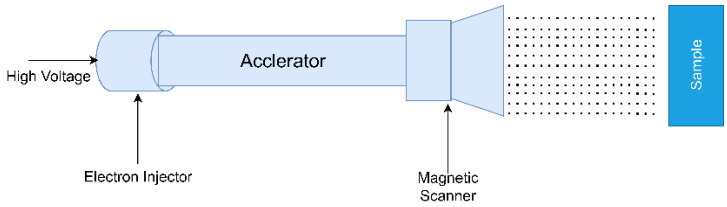

Figure 7: Electron beam's linear accelerator (LINAC)

2.4.2 Electron Beam Set-up

Electron beam with high energy after an accelerator can make great damage to DNA. Therefore, this eBeam center also treats food like Mango provided by Walmart, Inc. for pasteurizing and removing insects and pests from fresh products. Besides that, during electrons interact with water, the following oxidative/reductive radical species are formed:

$$0.7H_2O \xrightarrow{Ionizing\ Radiation} [0.27]e^-_{aq} + [0.28]\cdot OH + [0.06]\cdot H + [0.07]H_2O_2 + [0.27]H_3O^+ + [0.05]H_2$$

Electron beam with high energy after an accelerator can generate a large number of reactive species such as hydrated electron (e_{aq}^-), hydrogen radical ($H^\bullet$), and hydroxyl radical ($^\bullet OH$). These reducing and oxidizing agents play an important role to break down the carbon-fluorine bond based on the previous studies.

2.4.3 Dosage Measurement

Dosimeters were used to calculate the dose rate and get the required time of target dose. Four alanine dosimeters were placed in a line above the sample on top of the pipe, and one was placed under the pipe where the sample is located. (Figure 8)Each dose was read by EPR spectrometer Bruker e-scan and used to calculate the dose uniformity ratio

(DUR) of each sample. Dose received was confirmed via alanine dosimeters handled by the NCEBR staff dosimetrist.

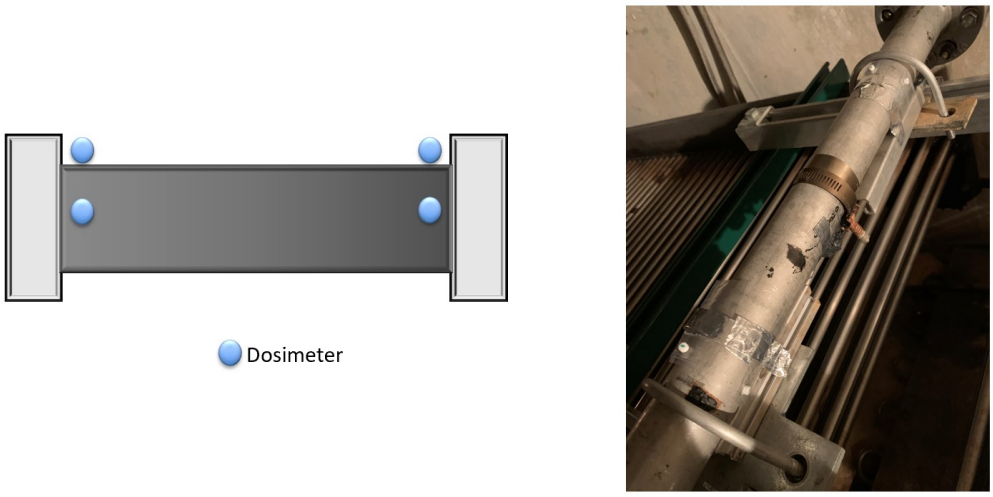

Figure 8: Alanine dosimeters for calculating dose rate

2.4.4 Possible Breakdown Pathway

At present, there have been many studies on the breakdown mechanism of PFOS/PFOA in different processes. For the degradation of PFOS and PFOA, there are mainly two aspects: one is the breaking of carbon-carbon bonds and carbon-fluorine bonds. The other is the location and path of the broken bond.

It was been noted that hydroxyl radicals play an important role in the removal of PFASs. Jin et al.[68] proposed the photochemical breakdown mechanism of PFOS induced by iron ions (Fe^{3+}). Perfluoro octane sulfonic acid forms a complex with Fe^{3+}, and under the excitation of UV light, a charge transfer process occurs from the ligand to the metal, producing Fe^{2+} ions and PFOS free radical $C_8F_{17}SO_3\cdot$. Perfluoro octane sulfonate free radical is unstable, and dislocation reaction will occur quickly to form perfluoroalkyl radical $C_8F_{17}\cdot$, the part of the removed SO_3 will soon be oxidized to sulfate (SO_4^{2-}), and

the generated Fe^{2+} can be re-oxidized to Fe^{3+} through the action of O_2, and then to realize the cycle of Fe^{2+} / Fe^{3+}. In an oxygen atmosphere, the perfluoro octane radical $C_8F_{17}\cdot$ reacts with hydroxyl radicals produced by the photolysis of Fe^{3+} ions in an aqueous solution to produce an unstable alcohol $C_8F_{17}OH$. The unstable alcohol $C_8F_{17}OH$ will remove HF to form $C_7F_{15}COF$, and after hydrolysis will form perfluorooctanoic acid. Under the same conditions, perfluorooctanoic acid will also form a complex with Fe^{3+}, and then the charge transfer process will occur, generating Fe^{2+} ions and unstable radical $C_7F_{15}COO\cdot$. The free radical $C_7F_{15}COO\cdot$ will continue to decarboxylate to form a short-chain perfluoro carboxylic acid radical $C_7F_{15}\cdot$ and repeat the above reaction path to gradually generate short-chain perfluoro carboxylic acid, and finally mineralize.

In addition, Qu et al.[69] found that hydrated electrons are the main factor affecting the degradation of PFOA, which can directly break the C-F bond adjacent to PFOA. Many hydrated electrons are generated in water, and the hydrated electrons directly interact with the fluorocarbon bond of PFOA to generate free radical $C_7F_{14}COOH$(Figure 9, reprinted with permission from Cui, 2020). After some series of defluorination and hydrolysis reactions, $C_6F_{13}COOH$ is generated and the next step is repeated (Figure 10) [70]. Thus, gradually degraded. Jin et al.[68] proposed a similar degradation mechanism in the study of degrading PFOS under vacuum ultraviolet light with a wavelength of 185 nm.

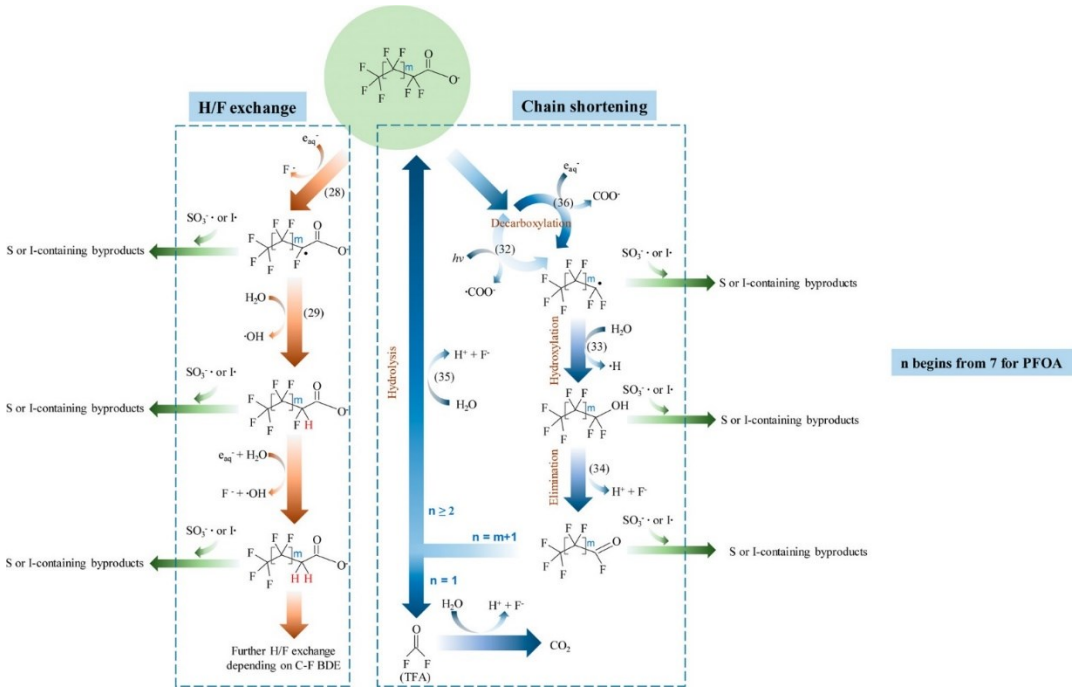

Figure 9: PFCAs breakdown with e_{aq}- possible pathways. Reprinted with permission from [54]

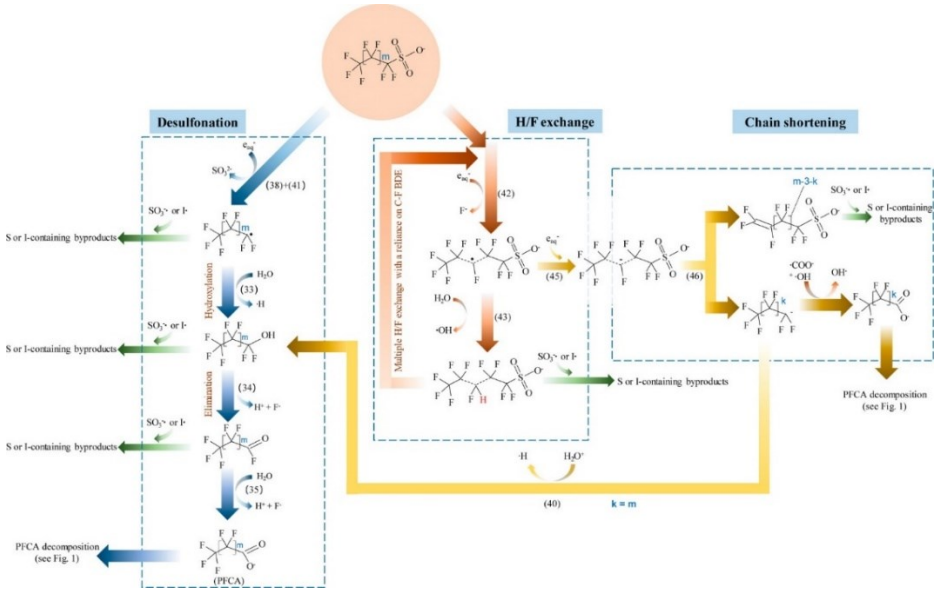

Figure 10: PFSAs breakdown pathway with e_{aq}^-. Reprinted with permission from [54]

CHAPTER III

RESEARCH METHODOLOGY AND APPROACH

This research topic will be mainly composed of five parts: chemical reagents and experiment set up design, experiment design, analytical method, and modeling method.

3.1 Chemicals and Reagents

All reagents related to solution preparation or were purchased from Sigma-Aldrich (St. Louis, MO) (Table 2). PFOS dissolved in Methanol for preparation of stock solutions or use as analytical standards were purchased from Wellington Labs (Guelph, Ontario). PFOA and PFHpA (50.0 μg/mL) in methanol for low lose and high dose experiments were also from Wellington Labs (Guelph, Ontario). High-density polyethylene bottles were purchased from VWR (Radnor, PA). Alanine dosimeters for dose mapping and reading absorbed doses were purchased from Bruker Scientific LLC (Billerica, MA).

Table 2: Chemicals and reagents for preparation of lab spiked sample and solid-phase extraction

Chemicals	**CAS NO.**	**Purity**	**Source**
Methanol	67-56-1	Analytical grade	Sigma Aldrich (St. Louis, MO)
PFOS	1763-23-1	Analytical grade	Wellington Labs (Guelph, Ontario)
PFOA	335-67-1	Analytical grade	Wellington Labs (Guelph, Ontario)
PFHpA	375-85-9	Analytical grade	Wellington Labs (Guelph, Ontario)
HPLC water	7732-18-5	HPLC grade	Sigma Aldrich (St. Louis, MO)
Ammonium hydroxide	1336-21-6	Analytical grade	Sigma Aldrich (St. Louis, MO)
Ammonium acetate	631-61-8	Analytical grade	Sigma Aldrich (St. Louis, MO)

3.2 Experiment Setup

All the low low-dose and high-dose experiments are done at Texas A&M University's National Center for Electron Beam Research (NCEBR). The Electron beam (eBeam) equipment has two vertically mounted 10 MeV, 15 kW eBeam linear accelerator. (Figure 11)

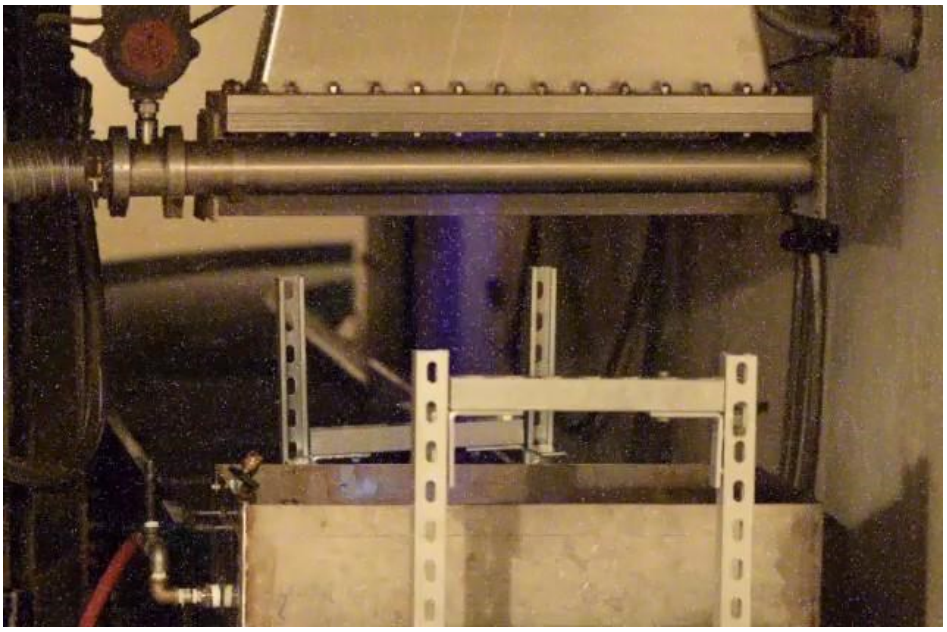

Figure 11: Electron beam horn

For this project, a high-dose experimental setup was designed and worked for both groundwater samples and soil samples. Figure shows how this system is designed. The aluminum sample tube can hold three sample boat which contains 100g water or soil at the same time. 3'' Condensate collection tube was also made from aluminum with a larger volume than the sample tube. Considering it is a sealed high-pressure system, there are two pressure relief valves on the tube connected sample tube and condensate collection tube. Thermocouples were tightened by the clamp.

For this project, a high-dose experimental setup was designed for both groundwater samples and soil samples. Figure 12, 13 shows how this system is designed. The aluminum sample tube can hold three separate sample boats which contains 100mL water or 100g soil. Additionally, a three-inch condensate collection tube was made from aluminum with a larger volume than the sample tube, to reduce pressure buildup within the system. Considering it is a sealed high-pressure system, there are two pressure relief valves on the tube connected sample tube and condensate collection tube. Thermocouples were tightened by the clamp.

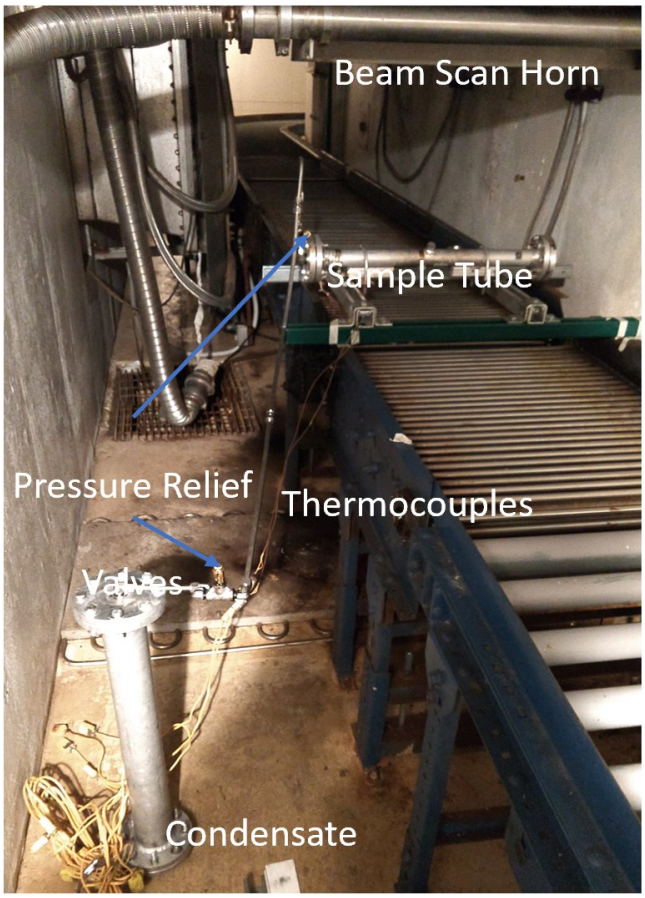

Figure 12: Treatments of field samples by high dose eBeam irradiation under different conditions

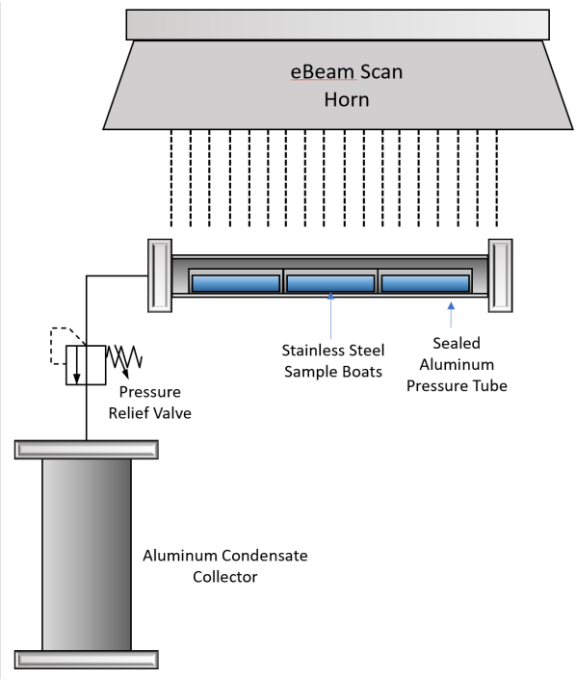

Figure 13: Schematic illustration of the high-dose eBeam irradiation setup.

The four clamps of pressure tube and condensate collector were sealed by high-temperature silicone gasket with thickness of 1/8". (Figure 14)

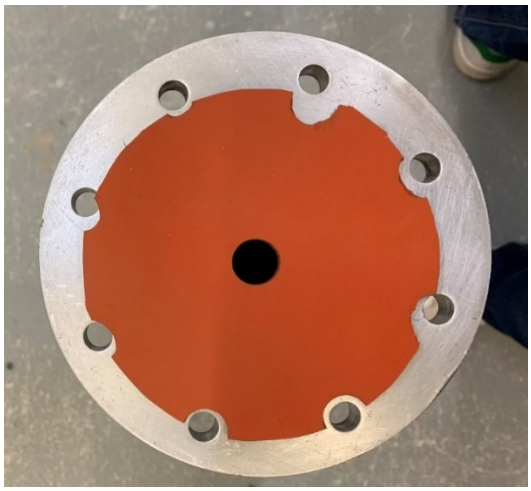

Figure 14: Silicon gaskets (1/8") for clamp sealing

Thermocouple was connected with the pressure tube and monitor control panel and pressed by hose clamp. (Figure 15) This system could record the temperature during the irradiation.(Figure 16)

Figure 15: Hose clamp for connection of K type thermocouples

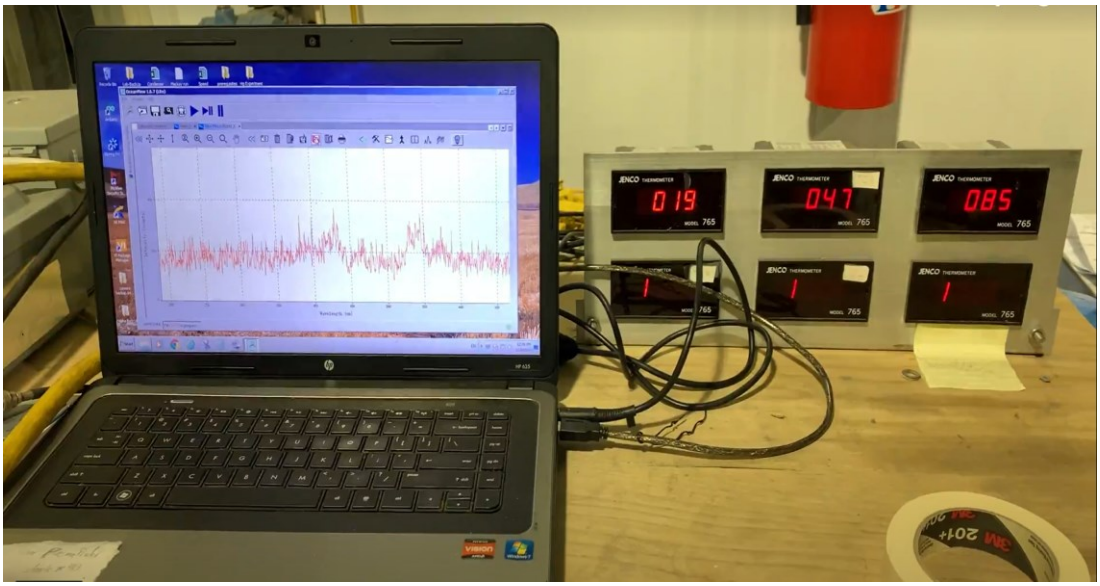

Figure 16: Temperature monitoring control panel for getting real-time change of temperature during eBeam irradiation.

3.3 Experimental Design

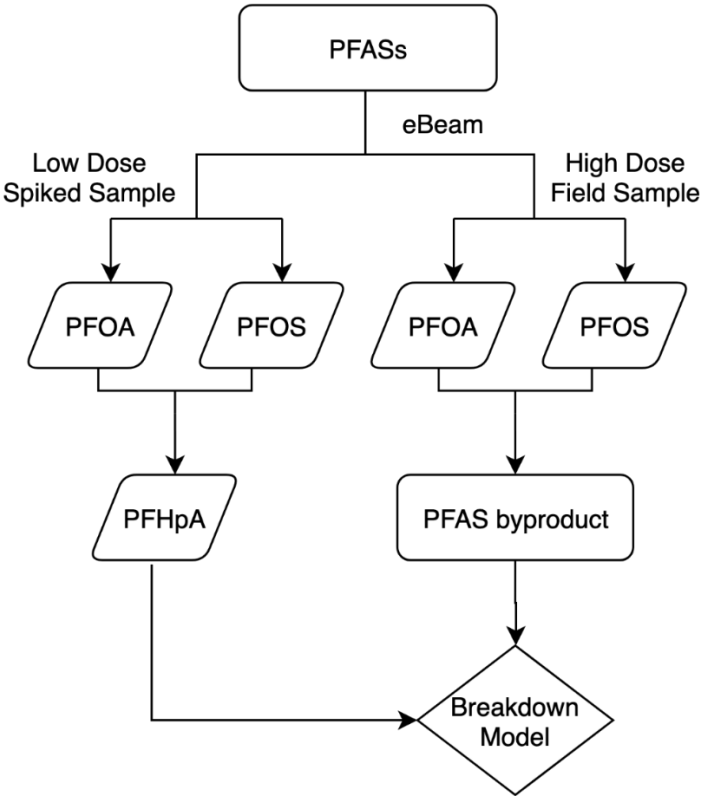

Figure 17: Experiment design flow chart

The experiments were designed as follows (Figure 17) to determine the effectiveness of eBeam irradiation in the removal of PFASs (i.e., PFOA, PFOS, and PFHpA) and to optimize the conditions that could achieve their maximum breakdown. Firstly, the low-dose portion of this research provided valuable insight into the minimum dose required to completely break down PFOA (50 kGy) and established that breakdown of PFOS would require much higher doses and possibly adjustment of the spiked sample conditions. Secondly, field samples including wastewater and soil were subject to get higher dosage irradiation: 250 kGy, 500 kGy, 1000 kGy, and 2000 kGy. Thirdly, as one

of the breakdown byproducts of PFOS and PFOA, PFHpA was chosen to get low-dose irradiation for modeling analysis.

3.3.1 Sample Collection

Field samples were sampling from Pennsylvania soil and Michigan water. Filed water samples were gathered in Pennsylvania. All samples will be collected in methanol washed, sterile, HDPE and to a lesser extent polypropylene sampling container. Only nitrile gloves will be used in the laboratory and when handling samples. All disposable sampling materials will be treated as single use. Decontamination of re-useable equipment will be performed using either Alconox, Liquinox or a solvent such as methanol. All final rinses will be performed using methanol. To avoid unnecessary sample manipulation the objective will be obtain a large volume of materials to support the proposed sample needs. Environmental samples will not be filtered in the laboratory. However, environmental sludge sludges can be expected to be mixed as necessary to prepare a homogenous sample to avoid unequal distribution of PFAS. If particle separation is required for the experiment, centrifugation followed by combining a solvent rinse of the particulate-containing centrifuge tube with the sample is proposed.

Samples will be shipped from the field /collection site to Texas A&M University (TAMU) by overnight courier on wet ice. TAMU will provide the sampler with the necessary sampling and shipping materials. A sample chain of custody form will be included in each sample shipment. The chain of custody forms will be scanned and stored electronically. An aliquot of the sample will be analyzed at the in-house laboratory. The sample designation will be affixed to the sample bottles for identification. The key to the

designation will be maintained electronically. The samples will be stored between 4 -7 °C for the duration of the project. In all experiments, control (un-treated samples) will be analyzed for their initial PFAS concentrations using both the in-house laboratory. The samples will be analyzed using the external commercial laboratory as needed.

3.3.2 Sample Preparation

All samples are divided into five classes: lab-spiked PFOS water sample, lab-spiked PFOA water sample, lab-spiked PFHpA water sample, field water sample, and field soil sample.

In preparing the lab-spiked samples for low-dose eBeam irradiation, 10.0 mg/L PFOS standard was used as the stock solution and diluted 10-time with methanol, followed by further dilution using HPLC water. Specifically, to obtain the experimental concentration, 1.0 mL of 1.0 mg/L PFOS was placed in high-density polyethylene (HDPE) bottle and added with 99.0 mL HPLC water. 100.0 mL of as-prepared 10 μg/L PFOS was divided into two 50.0 mL working solution and stored in 60 mL square HDPE bottles for future low-dose irradiation. As for the lab-spiked PFOA water sample, the same two-step dilution method was used to have 5.0 μg/L PFOA in water.

To prepare water samples of PFHpA for low-dose treatment, 100.0 μg/L PFHpA was diluted and used as the initial concentration. The effect of solution pH was studied at pH 13.0 and 6.0, which were prepared using 0.1 M NaOH and without pH adjustment, respectively. 50.0 mL of the solution was placed in HDPE bottles and purged with nitrogen to remove the dissolved oxygen. Afterward, the samples were sealed with parafilm, followed by eBeam irradiation studies at the facilities of the NCEBR.

Regarding the eBeam treatments for field samples from AECOM, the soil samples were added with NaOH for pH adjustment to get 13.0 and 7.0. 0.1 M sodium nitrate ($NaNO_3$) and 1 M sodium bicarbonate ($NaHCO_3$) were added to the field samples to improve the concentrations of aqueous electrons. The adjusted samples were dried down from 84% to 10% moisture in the oven about 24 hours at 75 ^oC (Fischer Scientific IsoTemp 500 Series).

All samples were stored at 10 ^oC in HDPE bottles and preparation was performed in the chemical fume hood. The spiked sample's concentrations were tested and confirmed by liquid chromatography-mass spectrometry (LC-MS) in IMAC lab at TAMU.

3.3.3 High-dose Setup Preparation

Cleaning procedures and leak tests were individually performed every time before radiation treatments to remove PFAS residues from the last experiment and to ensure proper sealing when pressure in the tubes increased. Briefly, 99.9% methanol was sprayed on the surface of the paper towel wadding, which was run through the sample tube and condensate collector about four times. Then, a new paper wadding with a clean methanol-rinsed wipe went through these reactors again. Finally, the sample tube was rinsed by about 10 mL of methanol.

Leak tests were performed by nitrogen gas to verify the tightness of the connections of different size tubes. The sample pressure tube was connected to a nitrogen bottle. Soapy water was applied to the connections, after increasing the pressure in the experimental setup by opening the nitrogen valve slowly. Bubbles would be formed if there is any leakage.

Three parallel field or spiked samples were placed in a pressure sample tube and treated with high-dose eBeam irradiation (500, 1000, and 2000 kGy). Two thermocouples were connected with the sample tube and control panel. Notably, the temperature was monitored to almost achieve 350 ^{o}C at 2000 kGy. Tap water was used to speed up the cool down the pressure sample tube and condensate collector, being very careful not to get any water on the connections to minimize contamination.

The field samples and condensates, found in the condensate tube, after irradiation were transferred into 60 mL HDPE bottles. All samples were labeled with the experiment date, eBeam dosage, and source, sealed using parafilm and stored in a cooler. Afterward, all samples were transferred to 10 ^{o}C refrigerator for storage until analysis could be conducted using SPE treatments.

Cleaning procedures and leak tests were individually performed every time before high-dose treatment to remove PFAS residues from the last experiment and avoid leakage when the temperature was higher than the water's boiling point. Briefly, 100% methanol was sprayed on the surface of the paper towel ball, which was run through the sample tube and condensate collector about four times. Then, a new paper ball with a clean methanol-rinsed wipe went through these reactors again. Finally, the sample tube was rinsed by about 10 mL of methanol.

Leak tests were performed by nitrogen gas to verify the tightness of the connections of different size tubes. The sample pressure tube (Figure 18, 19) was connected with a steel nitrogen cylinder. Soapy water was applied to the connection parts,

followed by the increasing pressure in the experimental setup by opening the valve slowly. Some bubbles would be formed if there is any leakage.

Figure 18: Test point A for leak test

Figure 19: Leak test of point B

Three parallel field samples were placed in a pressure sample tube and treated with high-dose eBeam irradiation (500, 1000, and 2000 kGy). (Figure 20)Two thermocouples were connected with the sample tube and control panel. Notably, the temperature was

monitored to almost achieve 350 ºC at 2000 kGy. Tap water was used to cool down the pressure sample tube and condensate collector. After that, the flange was opened, and the reaction boat was removed.

Figure 20: Michigan soil field sample after 2000 kGy ebeam irradiation

The field samples and condensates after irradiation were transferred into 60 mL HDPE bottles. All samples were labeled as the experiment date, eBeam dose, and source, sealed using parafilm and stored in a cooler(Figure 21). Afterward, all samples were transferred to 10 ºC refrigerator for further SPE treatments.

Figure 21: IDW soil sample after high dose treatment waiting for SPE

3.4 Analytical Method

3.4.1 Solid-Phase Extraction (SPE)

After eBeam treatment, all PFASs even PFOS concentration has a significant drop. To make sure most of the PFASs could be detected and the purity of the sample sent to LC-MS, all the spiked samples and field samples including the groundwater and soil were concentrated by Waters Oasis WAX vacuum cartridges (30 μm particle size, 1 cc) (Figure 22).

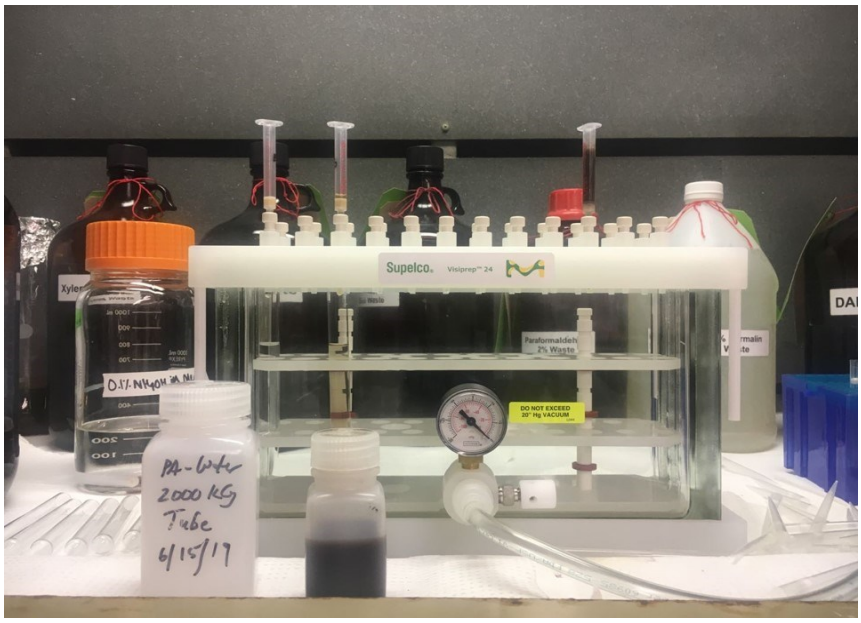

Figure 22: Solid phase extraction (SPE) manifold for concentrate and purify sample

The extraction of soil samples was centrifuged before extraction due to too many large particles. Firstly, 10 mL of methanol was added to the sample tube containing 1.0 g soil sample (in four replicates), and vortexed then sonicated. 300 mL of pure water was transferred to the beaker (a total of 330 mL) which could avoid PFOA goes with methanol when load sample through cartridge. Nitrogen evaporator was used to purge nitrogen for keep no oxygen atmosphere and then concentrate 330mL sample to 10mL.

The purified process following the procedures below. The SPE column was conditioned with 0.1% ammonium hydroxide in methanol three times. And then 100% methanol 3 mL total was used to condition the column again. Each sample was vortexed by 5-10 seconds at a speed of 10 for MINI VORTEXER to ensure uniformity. 1 mL sample was loaded and then washed with 1 mL 25 mM ammonium acetate with a regular vacuum setting (10’’-20’’ Hg Vacuum). Next, the cartridge was dried with low vacuum for 3-5

minutes. Fresh sample collection tubes were placed under SPE column. The vacuum manifold's ports were switched to an unused state. 1.0 mL 0.1% ammonium hydroxide in methanol was used to elute under a low vacuum. The sample was immediately transferred from tube to 1.5 mL vial and covered with parafilm. Vacuum manifold setup was removed from the hood. All the samples were stored at 4 ºC on refrigerator until LC-MS/MS analysis.(Figure 23)

Figure 23: Spiked sample for low-dose after solid-phase extraction

3.4.2 LC-MS

All targeted PFASs concentration was determined by Integrated Metabolomics Analysis Core (IMAC) at Texas A&M University and SGS-AXYS in British Colombia, Canada. The HPLC system (Vanquish, Thermo Scientific) was equipped a binary pump. A direct infusion rate of 5 µL/min was used for selective reaction monitoring (SRM) to get the optimal MS conditions. 10 µL was required to inject, using an 8-minute solvent gradient method to adjust to 30 °C. And The flow rate was set as 0.5 mL/min.

3.5 Modeling Method

3.5.1 Pseudo First Order Kinetic Model

Assume a linear rate constant model: the reaction rate is negative linear relation to the first power of the concentration of the reactant, which means a change in PFOS is proportional to the concentration of e^- and PFOS linearly.

$$dN_{PFOS} = -K_1 \cdot {N_{PFOS}}^a \cdot {N_{e^-}}^b$$

Here, dN_{PFOS} (ng/mL) is the change of PFOS concentration; K_1 is the constant coefficient of first-order chemical kinetic; ${N_{PFOS}}^a$ (ng/mL) is the initial PFOS concentration before radiation; ${N_{e^-}}^b$ is the concentration of electron.

Assuming the number of electrons is proportional to dose.

$$N_{e^-} = K_2 \cdot Dose$$

Where ${N_{e^-}}^b$ is the concentration of electron; K_2 is the ratio of electron concentration to dose; Dose (kGy) ranges from 0 to 2000 in this case. Applying the Eq.(2) to the first one, then

$$dN_{PFOS} = -K_1 \cdot K_2 \cdot N_{PFOS} \cdot \mathrm{D}$$

Introducing

$$K_3 = K_1 \cdot K_2$$

We find:

$$\frac{dN_{PFOS}}{\mathrm{dD}} = -K_3 \cdot N_{PFOS}$$

$$\frac{dN_{PFOS}}{N_{PFOS}} = -K_3 \cdot \mathrm{dD}$$

Furthermore, integrate the equation.

$$\int \frac{dN_{PFOS}}{N_{PFOS}} = \int -K_3 \cdot \mathrm{dD}$$

$$\ln N_{PFOS} \Big|_{0}^{N_{PFOS}(D)} = -K_3 \cdot (\mathrm{D} - 0)$$

$$\ln \frac{N_{PFOS}(D)}{N_{PFOS}(0)} = -K_3 \cdot \mathrm{D}$$

Where $\frac{N_{PFOS}(D)}{N_{PFOS}(0)}$ shows the degradation rate.

Hence, the PFOS concentration can be expressed in terms of

$$N_{PFOS}(D) = N_{PFOS}(0)e^{-K_3 \cdot \mathrm{D}}$$

We could also write as follows,

$$PFOS_{remaining} = PFOS_{initial} \times e^{-k \times Dose}$$

3.5.2 Model Development

After eBeam irradiation on different doses (0 kGy, 500 kGy, 1000 kGy, and 2000 kGy), the mass of PFOS was supposed to meet the mass of balance. A kinetic model about chemical reaction rate and the ratio of different reactions is developed and validated.

Assume the following model:

$$\frac{dN_{PFOS}}{dt} = - N_{PFOS} \cdot b_1 D$$

$$\frac{dN_{PFOA}}{dt} = - N_{PFOA} \cdot b_2 D + N_{PFOS} \cdot r_{8\_S} b1D$$

$$\frac{dN_{PFHpS}}{dt} = - N_{PFHpS} \cdot b_3 D + N_{PFOS} \cdot r_{8\_C} b_1 D$$

$$\frac{dN_{PFHpA}}{dt} = - N_{PFHpA} \cdot b_4 D + N_{PFOS} \cdot r_{8\_CS} b_1 D + N_{PFOA} \cdot r_{8a\_C} b_2 D + N_{PFHpS} \cdot r_{7\_S} b_3 D$$

$$\frac{dN_{PFHxS}}{dt} = - N_{PFHxS} \cdot b_5D + N_{PFHpS} \cdot r_{7\_CS}b_3D$$

$$\frac{dN_{PFHxA}}{dt} = - N_{PFHxA} \cdot b_6D + N_{PFHpS} \cdot r_{7\_CS}b_3D + N_{PFHpA} \cdot r_{7a\_C}\, b_4D + N_{PFHxS} \cdot r_{6\_S}b_5D$$

$$\frac{dN_{PFPeS}}{dt} = - N_{PFPeS} \cdot b_7D + N_{PFHxS} \cdot r_{6\_C}b_5D$$

$$\frac{dN_{PFPeA}}{dt} = - N_{PFPeA} \cdot b_8D + N_{PFHxA} \cdot r_{6a\_C}b6D + N_{PFHxS} \cdot r_{6\_CS}b_5D + N_{PFPeS} \cdot r_{5\_S}\, b_7D$$

$$\frac{dN_{PFBS}}{dt} = - N_{PFBS} \cdot b_9D + N_{PFPeS} \cdot r_{5\_C}b_7D$$

$$\frac{dN_{PFBA}}{dt} = - N_{PFBA} \cdot b_{10}D + N_{PFBS} \cdot r_{4\_S}\, b_9D + N_{PFPeA} \cdot r_{5a\_c}b_8D + N_{PFPeS} \cdot r_{5\_CS}b_7D$$

Here, dN_{PFASs} (ng/mL) is the change of PFASs concentration; $b_1 – b_{10}$ is the constant coefficient, is the same as K in pseudo first order kinetic model ; N_{PFOS} (ng/mL) is the initial PFASs concentration before radiation; r is the weight of different; D is dose rate kGy/s.

$$C_{n+1}S \rightarrow C_nS \rightarrow C_{n-1}S$$

$$C_{n+1}\& \; C_{n+1}S \rightarrow C_n \rightarrow C_{n-1}$$

3.5.3 Comparison between Experimental Data and Simulated Results

MATLAB was used to simulate the difference between experimental data and simulated results. The difference is a one-dimensional array with three parameters calculated by three parts. Firstly, the result of simulated results minus experimental data is calculated for further use.

$$\Delta C = C_{mod} - C_{exp}$$

Where C_{mod} is modeling concentration, C_{exp} is experimental concentration.

The difference between experimental data and simulated results was given by:

[diff2,diff3,diff]

Where diff2 is least squares in linear space, diff3 is the least squares in log space, diff is the weighted sum of the first two parts.

$$diff2 = \frac{\sqrt{(\sum \Delta C^2)}}{\left(Max(C_{exp})\right)}$$

$$diff3 = \frac{\sqrt{(\sum \ln \Delta C^2)}}{\ln\left(Max(C_{exp})\right)}$$

$$diff \ = \ 0.25 * diff2 + 0.75 * diff3$$

3.5.4 Goodness of Fit

Suppose the initial temperature is 25 ℃, the initial dosage is 0 KGy as no treatment control group. The model concentrations based on the ODE45 model with various parameters were calculated, this function then compares the model to experimental values the output is the goodness of fit and can be used in a function minimization.

[tout,yout] = ode45(@(t,y)ODEFUN_PFAS(t,y,params),time,initconc);

ODEFUN_PFAS(t,y,params) is the modeling function to be solved.

Where tout is modeling time, the column 1 to 10 in yout is modeling concentration, the last column in yout is dose.

Pseudo code as follows:

%dose Conc is modeling data, Doses ng_D is experimental data

diff = findPFASdiff(dose,Conc,Doses,ng_D);

```
        if
params(1)>0.9999|params(2)>0.9999|params(3)>0.9999|params(6)>0.9999  %
upper bound
           diff = diff*100
        end
        if find(params<0) % bound positive
           diff = diff*100
```

CHAPTER IV

RESULTS AND DISCUSSION

4.1 Breakdown of PFOA and PFOS at Low Dose of eBeam Irradiation

Chemical reaction efficiency is affected by some common operating conditions such as pH. Key factors affecting the efficiency are designed to do some control experiment for finding the optimal reaction condition and scale it up. It has been demonstrated that with the nitrogen saturation, hydrated electron (e_{aq}^-), hydrogen radical (H•) were main reducing agents in the solution.[71] This could be due to the reaction of O_2 with e_{aq}^- and H•. (Eq.) With the decrease amount of oxygen, e_{aq}^- and H• will increase and result the fasten breakdown process. Ma et al. have suggested that the lower oxygen concentration significantly increased the PFOA and PFOS degradation rate. [71]

$$e_{aq}^- + O_2 \rightarrow O_2^{\bullet -}$$

$$H\cdot + O_2 \rightarrow HO_2\cdot$$

In this study, to determine the optimal experimental condition and whether the initial pH would influence the reaction, the spiked PFOA and PFOS were treated at pH 6.0 and 13.0 without oxygen. Furthermore, dosage catalyst the degradation process of PFASs. For investigating the effect of electron beam dose of 0-75 kGy in aqueous solution for the decomposition of PFASs, the lab-spiked PFOS water sample (100.0 μg/L), lab-spiked PFOA water sample (100.0 μg/L), lab-spiked PFHpA water sample (100.0 μg/L) were prepared by HPLC water.

Figure 24 shows the concentration change of laboratory spiked PFOA and PFOS water samples at 0, 5, 10, 25, 50 and 75 kGy. The volume of water sample did not change at low dose because the temperature during irradiation did not get 100 °C. Therefore, concentration was tested using LC-MS rather than mass could notify the amount of PFOA and PFOS. We note that PFOA was breakdown at 5 kGy with pH adjustment. Specifically, 8.19% breakdown of PFOA was removed in lab-spiked water (Figure) without any pH adjustments at 75 kGy. At 75 kGy, the degradation of PFOA reached the highest efficiency 14.61% at pH 13.0. In general, Figure shows the breakdown process occurring rapidly with higher dose. One important feature noted by this figure is the presence of OH^- has good influence on decompose PFOA.

Considering the experimental error and uncertainty, there's no significant difference of PFOA degradation percentage at different alkalinity with low dose irradiation. Higher decomposition ratio was observed with the increase of dose.

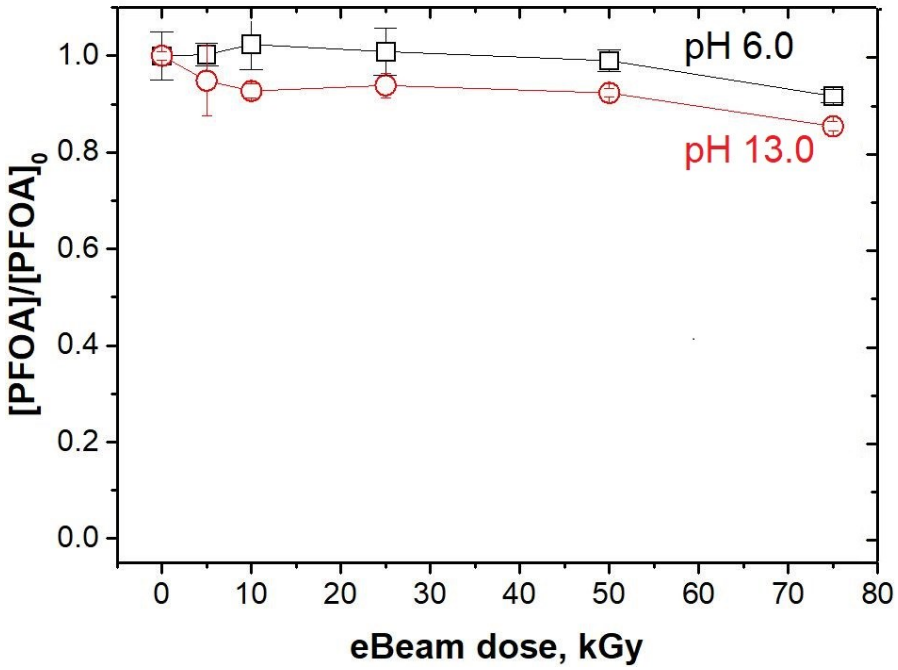

Figure 24: eBeam dose profiles for PFOA breakdown, reaction conditions: [PFOA]= 100.0 µg/L, pH = 6.0 or 13.0, without oxygen, electron beam dose =0,5,10, 25, 50 75 kGy

Preliminary results of PFOA shows that low dose irradiation could lead the destruction at PFOA. Previous study showed that PFOS has stronger stability and bioaccumulation. Saerom's research showed that reactions with PFOA initiated much greater activity than PFOS, PFOA could be oxidized by persulfate at 50 °C after treatment of 72 hours while PFOS will not be decomposed even with higher activation temperature and longer time.[72] It indicated that PFOS was more resistant to decompose.

By applying the same experiment design with PFOS, similar results showed the relationship of degradation efficiency with eBeam dose. (Figure 25) Decomposition of PFAS is a pH-dependent process. Figure shows that the effect of pH for PFOS (100.0 µg/L) breakdown by electron beam. After 75 kGy eBeam irradiation at pH 6.0 and pH

13.0 without oxygen treatment, the corresponding breakdown percentages of PFOS were 13.4% and 18.14% respectively. Consequently, PFOS degraded faster with higher pH.

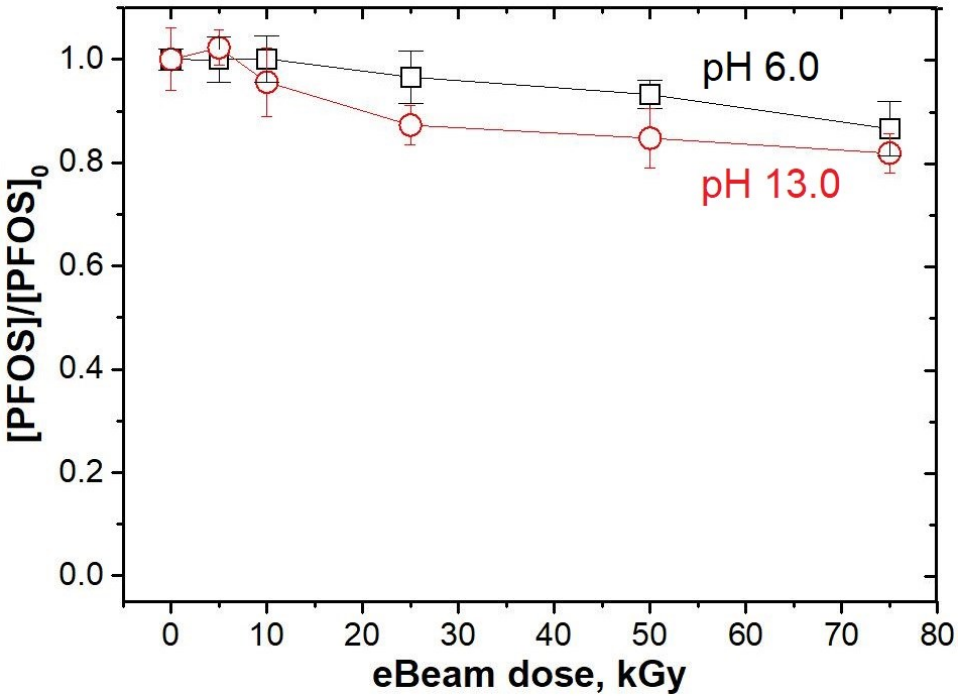

Figure 25: Reduction of PFOS (100.0 µg/L) at pH = 13.0 or 6.0 with nitrogen purging at different ebeam dose

It is noteworthy that, pH values of the matrix have effect on the generation of hydrated electrons. The increased reduction of PFOA and PFOS had been shown to be related to the electron beam dose and pH values. It has been demonstrated that alkaline pH condition results in the presence of more hydrogen electrons. Many researchers had shown that how the alkalinity effect decomposition due to the catalyzed mechanism of hydrogen electrons. [73]

$$e_{aq}^{-} + H^{+} \rightarrow \cdot H$$

$$OH^{-} + \cdot H \rightarrow e_{aq}^{-} + H_2O$$

Gu et al. [74] has investigated that removal percentage was increased from 60.4% to 91.1% while pH increase from 6.0 to 9.0 in VUV/sulfite system. Increasing pH to 13.0 also led to the high breakdown percentage to 88.1% at 500 kGy eBeam remediation.[71] Although many researchers reported the positive effect of higher pH on PFASs especially PFOA or PFOS, there's not a significant change of different pH in this study. This may be because the irradiation is not high enough. The results demonstrated that 75 kGy is not enough to fully breakdown PFOA and PFOS.

4.2 PFHpA Degradation by Low-dose eBeam Irradiation

To investigate the effect of water components on PFAS breakdown by eBeam irradiation, different amounts of bicarbonate, nitrate, and fulvic acid were pre-added into the solutions of PFHpA, a representative degradation product of PFOA/PFOS in different AOP/ARP processes. 50 mL of the PFHpA solution (100.0 μg/L) was placed in HDPE bottles and purged with nitrogen to remove the dissolved oxygen. Figure 26 shows that decomposition efficiency was 100% at 50 kGy, pH 13.0 without oxygen at different concentrations of nitrate ion (0, 5, 10, 15, and 20 mg/L). Figure shows that PFHpA reduction in laboratory spiked sample when exposed to 50 kGy. The decomposition efficiencies of PFHpA at various alkalinity (0, 25, 50, 75, and 100 mg/L) all were 100%. It was shown that PFHpA (100.0 μg/L) reduction in laboratory spiked sample when exposed to 50kGy. The decomposition efficiencies of PFHpA at different fulvic acid concentration (0 μg/L, 25 μg/L, 50 μg/L, 75 μg/L, 100 μg/L) all were 100%.

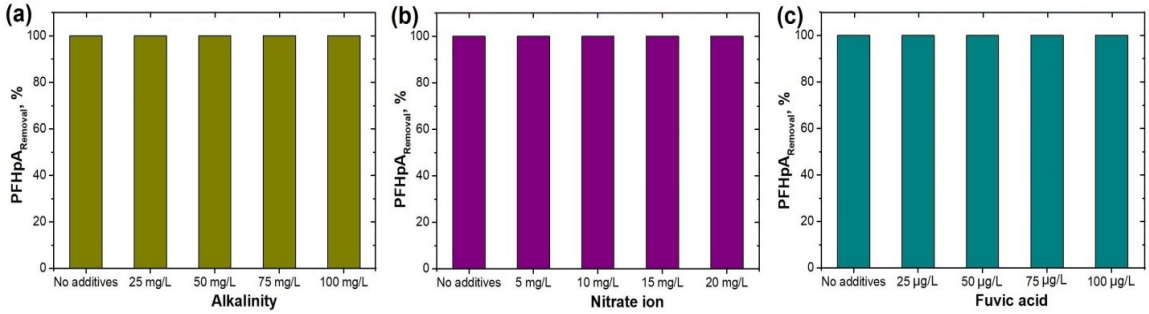

Figure 26: PFHpA (100.0 µg/L) degradation under different concentrations of (a) bicarbonate (HCO_3^-) (b)Nitrate ion (NO_3^-) and (c) Fulvic acid ($C_{14}H_{12}O_8$) with pH =13.0 without oxygen at 50 kGy dose eBeam irradiation

The presence of HCO_3^- in solution might inhibit PFHpA reduction as a result of reaction with a typical oxidation hydroxyl radical (•OH). [75] As the Equation shows the hydrogen carbonate (H_2O_2) and carbonate radicals were formed.

$$HCO_3^- + \bullet OH \rightarrow CO_3^{\bullet -} + H_2O_2$$

$$CO_3^{\bullet -} + H_2O_2 \rightarrow HCO_3^- + O_2^{\bullet -} + H^+$$

With the increase of concentration of HCO_3^- in solution at pH 13.0, more and more •OH was reacted. However, this study's results demonstrated that enhancement in the concentration of HCO_3^- would not inhibit the removal of PFHpA.

Nitrate ion (NO_3^-) is also a kind of oxidizing species which may consume hydrated electrons (e_{aq}^-). The following reaction mechanism has been proposed as the mechanism of e_{aq}^- transfer in alkane solutions[76].

$$e_{aq}^- + NO_3^- \rightarrow NO_3^{\bullet -}$$

This reaction is in good agreement with increasing nitrate ion driving the equation to right side, and thus led to a less e_{aq}^- in solutions. Based on the experiment study, nitrate

ion at pH 13.0 in PFHpA spiked sample will not have negative effect on PFHpA breakdown.

Fulvic acid ($C_{14}H_{12}O_8$, FA) is a major component in natural waters.[77] To further apply electron beam technology into natural waters or soil matrix, it is needed to investigate the effect of FA on PFAS decomposition efficiency. The literature on identify FA impact on adsorption of PFOS proved that FA increasing the efficiency via hydrophobic and electrostatic mechanisms.[78] Preliminary results indicate 100 µg/L FA will not repel the reduction process.

Several studies have shown that pH is an important influencing factor during electron beam irradiation. Because the change of the pH of the solution will affect the concentration of the active particles generated by the irradiation in the solution.[79] In Ma's study, as the initial pH increases, the degradation efficiency of PFOS and PFOA continues to increase[71]. PFOS and PFOA have the highest degradation efficiency at pH 13.0. Free radicals e_{aq}^- and H• produced by irradiating the aqueous solution can be converted into each other.[71]

Previous study on pH impact on PFOA/PFOS breakdown via electron beam shows that there's not a very significant catalyzation with pH enhancement. Furthermore, PFHpA was taken to investigate the relationship of pH value with degradation percentage.

Figure 27 shows that the concentration of PFHpA was rapidly decomposed with the increase of eBeam dose. The highest breakdown percentage was 94.97% with the lowest PFHpA concentration of 2.93 µg/L at pH = 13.0 with the dosage of 75 kGy. The decomposition efficiencies were 23.28%, 48.72%, 79.12%, and 94.50% at the absorbed

doses of 5, 10, 25, and 50 kGy. The decomposition efficiency was 12.7% at pH 6.0 with nitrogen purging compared. It shows a dramatic increase of breakdown percentage with the increase of pH. This was supported by the Ma's research[71] that degradation rate of PFOS achieved highest at pH 13.0.

It was noted by Figure 28(b), the PFHpA reduction at low-dose satisfied the pseudo first order kinetic model. The concentration of the PFHpA decreased exponentially as the dose increases.

$$\ln \frac{N_{PFHpA}(D)}{N_{PFHpA}(0)} = -\mathrm{K} \cdot \mathrm{D} + \mathrm{b}$$

Where $N_{PFHpA}(0)$ (ng/mL) is the initial PFHpA concentration before radiation, $N_{PFHpA}(D)$ (ng/mL) is the PFHpA concentration after radiation, $\frac{N_{PFOS}(D)}{N_{PFOS}(0)}$ shows the degradation rate.

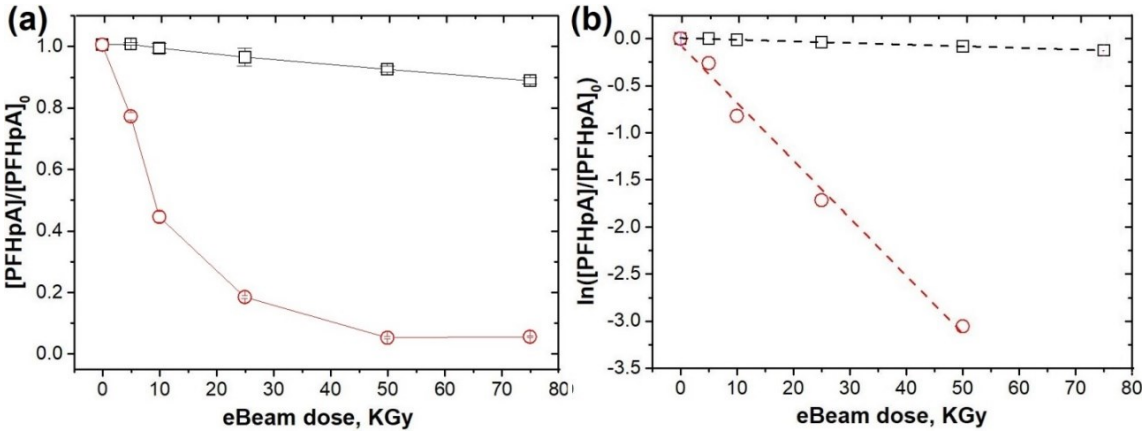

Figure 27: Removal of PFHpA by different doses of eBeam irradiation at pH 13.0 or pH 6.0 in water, (experimental conditions: [PFHpA] = 100.0 µg/L, eBeam doses = 0, 5, 10, 25, 50, and 75 kGy, with nitrogen purging).

The difference of PFHpA and PFOA/PFOS at different pH might because these samples got the eBeam at different labs. PFOA/PFOS got the standard treatment on the conveyor

belt at National Center for Electron Beam Research. Spiked PFHpA sample was irradiated at Sterigenics in California. One possible reason for this is pH effect will not be significant at low dose irradiation.

4.3 Field Water and Soil Sample after High Dose Remediation

Field water and soil samples were exposed to high dose electron beam remediation from 500 kGy to 2000 kGy with dose rate of 17.19 kGy/s . Previous study showed that high pH value has positive effective on spiked PFOA and PFOS water. However, field sample were never done before to prove the efficiency of PFASs reduction under electron beam. To elucidate the eBeam contributed for removal PFASs in water and soil matrix, this part studied the Pennsylvania groundwater and the Michigan soil samples with initial high PFOS concentrations. Table 3 shows that the initial concentration of PFOS in water sample was 38500 ng/L and PFOA of 1120 ng/L.

Table 3: Concentration of PFASs in Michigan groundwater after 0, 500, 1000, and 2000kGy eBeam irradiation with no pH ajustment (measured at SGS)

DOSE	0	500	1000	2000
Start Volume(mL)	100	100	100	100
REMAINING VOLUME(ML)	100	89	69	24
UNITS	ng/L	ng/L	ng/L	ng/L
PFNS	84.1			
PFNA		99.5	68.1	71.9
PFOS	38500	21900	16700	19400
PFOA	1120	944	1470	2150
PFHPS	712	829	737	1020

Table 3: Continued

DOSE	0	500	1000	2000
PFHPA	531	4170	2530	7270
PFHXS	5030	5820	5340	8610
PFHXA	18400	5880	15800	12000
PFPES	746	918	968	1770
PFPEA	5180	2570	7410	9850
PFBS	538	702	906	1910
PFBA	5030	1660	6550	8760

From the thermal couple data (Figure 28, reprinted with permission from Rodi, 2019)and the volume of water sample in sample tube, water evaporation was required to consider due to the temperature goes to 100^{o}C. Table 3 indicates that only 24 mL remaining in sample tube with initial volume is 100 mL. Therefore, concentration of PFAS was not performed the decompose efficiency. Consider this high-dose system was a closed system, mass for LC-MS targeted PFAS in field sample was calculated to show the decomposition efficiency. For example, the mass of PFOS in sample tube plus the PFOS mass in condensate collector is the total mass after eBeam irradiation, this number would be compared the initial mass which demonstrate the breakdown percentage.

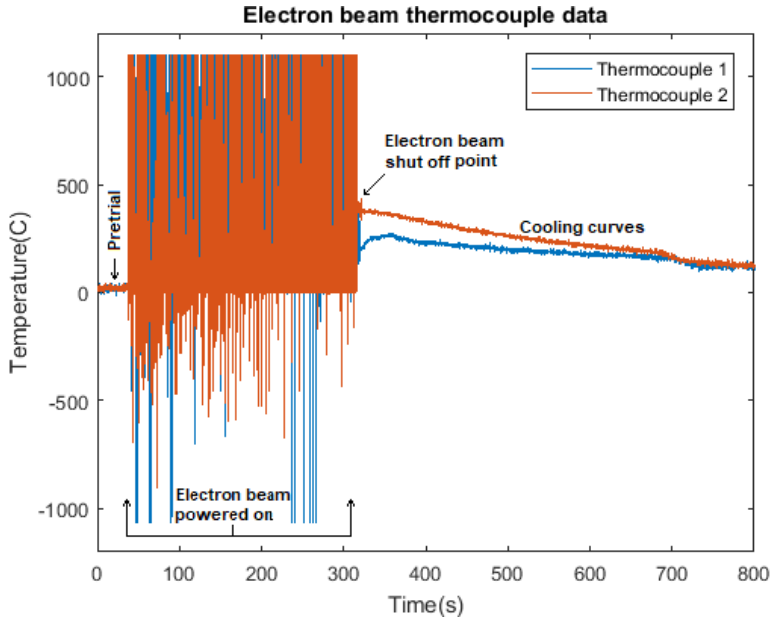

Figure 28 : eBeam thermo data at 2000 kGy irradiation. Reprinted with permission from [80]

Each field sample was sent to TAMU lab and commercial lab SGS-AXYS in Canada for LC-MS. Figure 29 shows the results of two different lab, it has been observed that lowest PFOS residue percentage based on SGS results was 12% at absorbed dose of 2000 kGy. This is consistent with the lab-spiked PFOS sample that enhancement of dose drives to higher removal efficiency. As shown in Figure 29, the residue percentages of PFOS of expose to 0, 500, 1000, and 2000kGy eBeam without pH adjustment were 100%, 36%, 24% and 12%. PFOS was rapidly degraded until 1000 kGy, the slope between residue percentage and eBeam dose was flatten after 1000 kGy.

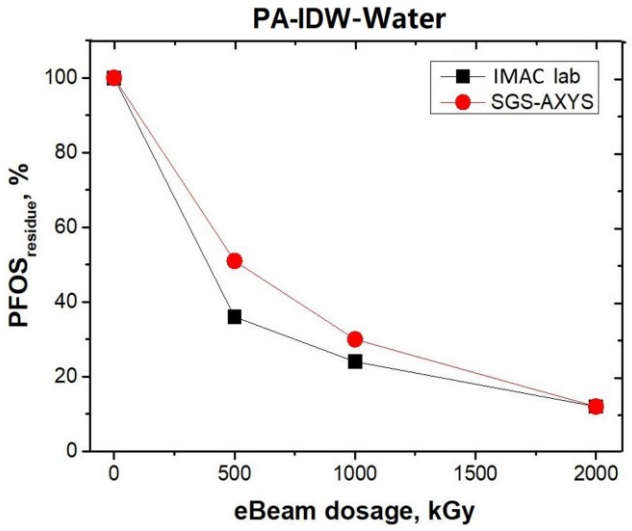

Figure 29: Residue percentage of PA-IDW-water with high eBeam dose treatment (0, 500, 1000 and 2000 kGy)

Figure 30 that shows the PFOA and PFOS breakdown percentages in Michigan soil sample at various doses. PFASs concentration remaining in the sample vessel, it has been observed that PFOS was more difficult to decompose until 1000 kGy. At 2000 kGy, PFOA and PFOS were almost fully removed, the decomposition efficiencies were 98.8% and 98.6%.

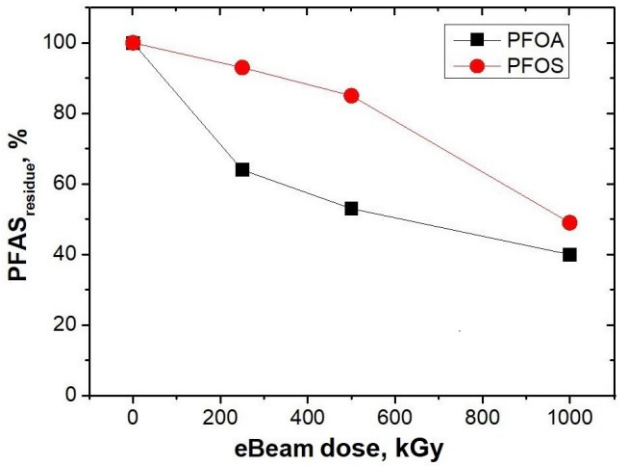

Figure 30: PFOA and PFOS breakdown in MI-IDW soil sample at various dose of 0, 250, 500, 1000 and 2000kGy. (Measured by SGS)

4.4 Kinetic Model Analysis

At present, there have been many studies on the degradation mechanism of PFOS and PFOA in different degradation processes. For the degradation of PFOS and PFOA, there are mainly two aspects: one is the breaking of carbon-carbon bonds and carbon-fluorine bonds. The other is the location and path of the broken bond. To investigate how PFOS defluorinate and the percentage of different pathway, kinetic model was required to calculate the constant at each reaction.

At 500 kGy, an increase in PFHpA and PFHxS is observed, this result suggested that the possibility of PFHpA was from PFOA or PFOS, PFHxS was from PFOS. (Figure 31)The increase of PFOA, PFPeA, PFHxA, and PFBA from 500 to 1000 kGy was observed. This indicated that the defluorinate of PFSA to eliminate F atom and then shorten the chain. In general, the mass of all PFAS component in field sample were decreased compared with initial amount.

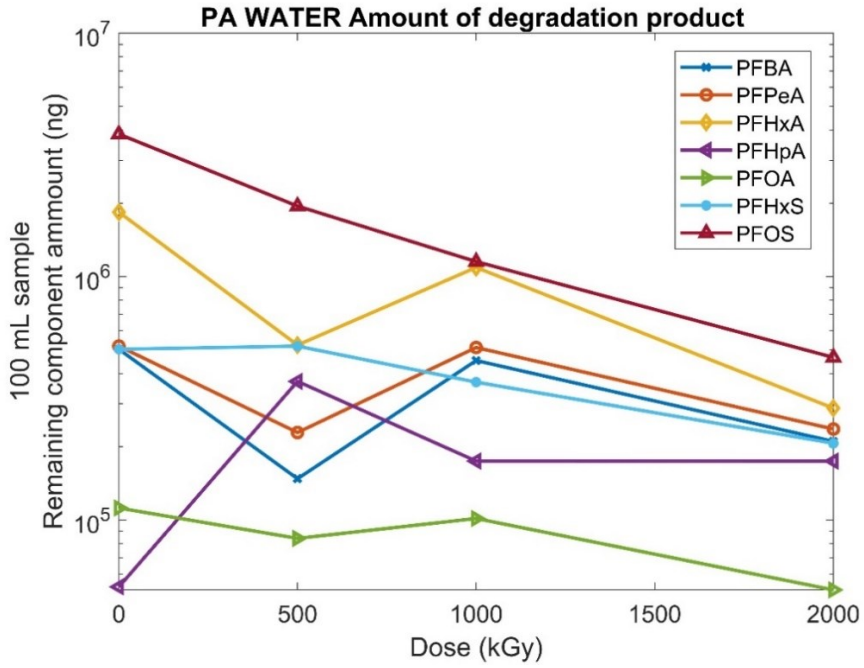

Figure 31: Profile of PA-WATER decomposition product with use of 0, 500, 1000, 1500, 2000 kGy eBeam irradiation

As shown in figure 32, PFPeA and PFHxS in soil sample increased while other components were breakdown. These results agree with the change of product mass in water sample. It is observed that PFPeA and PFHxS decrease followed increase after 200 kGy. After these increases, all breakdown products continue to degrade. At 1000 kGy, the mass of PFOA in sample tube decreased from 3793.49 ng to 1534 ng, in which 40.44% PFOA was removed. PFOS showed the least amount of breakdown in this sample group at 50.74% destruction.

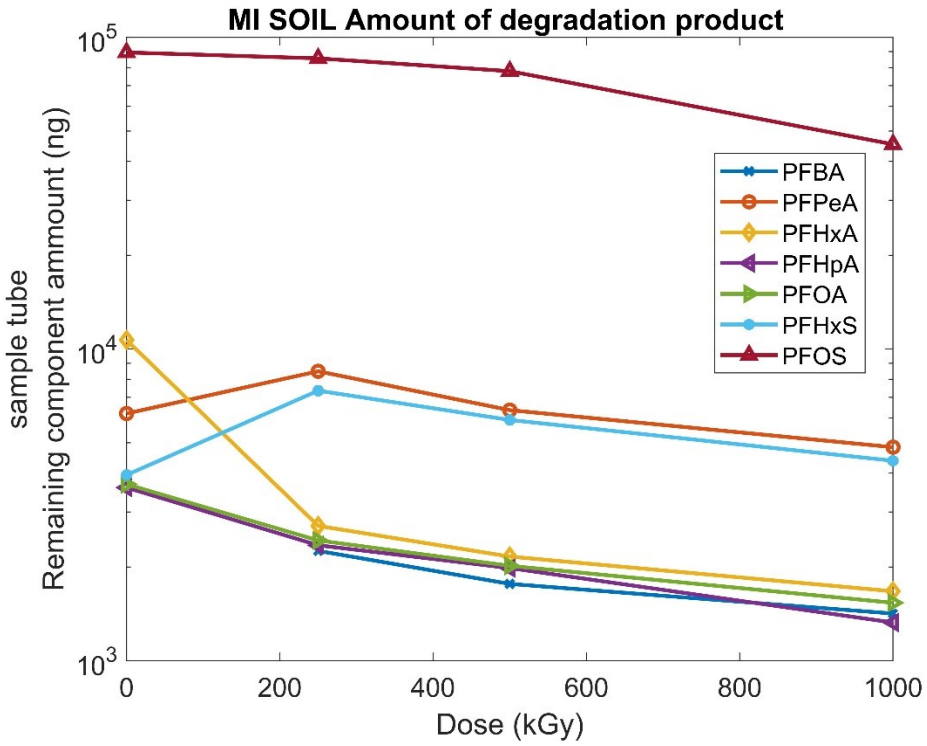

Figure 32: The amount of MI-SOIL degradation product at 0, 500, 1000, 1500, 2000 kGy eBeam irradiation

As shown in figure 33, implying that reaction equations to kinetic model, breakdown of C-F bonds on PFHpA for production of F^-. It was demonstrated that rate constant k of PFHpA at pH 6.0 is – 0.0016. After the linear fitting, breakdown of PFHpA at 0, 5, 10, 25, 50, 75 kGy satisfied the pseudo first kinetic order. Concentrations of the PFHpA degradation rates at low dose are typically increased with the enhancement of pH. At pH = 13.0, the rate constant k increased to – 0.0429, this result consistent with low pH that the fitted figure is a line.(Figure 34)

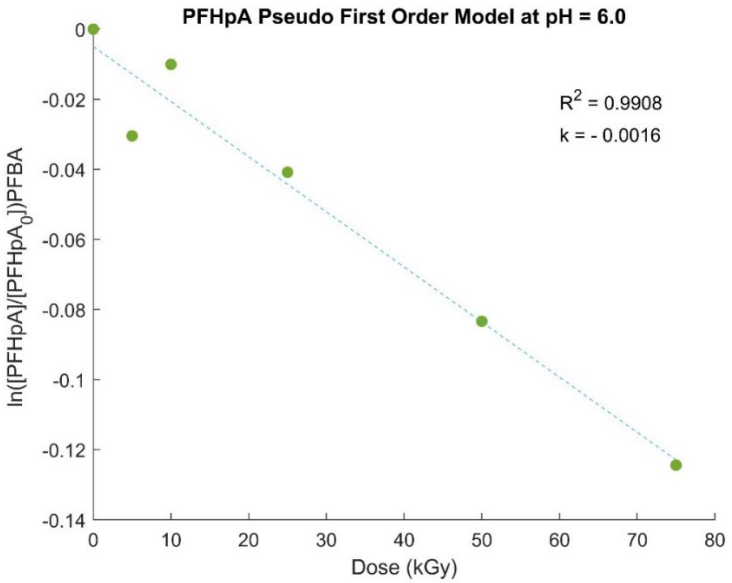

Figure 33: Kinetic model of PFHpA at initial concentration 100 (µg/L) under eBeam doses of 0, 5, 10, 25, 50, and 75 kGy

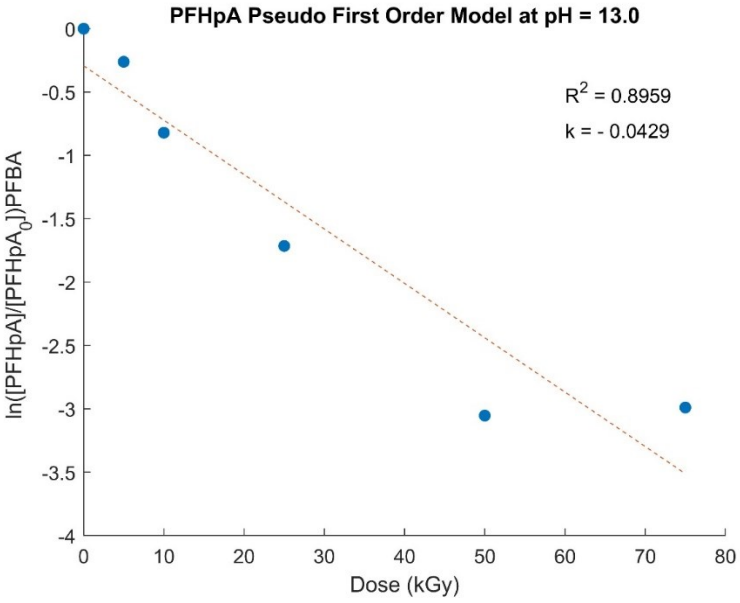

Figure 34: Pseudo first order kinetic of PFHpA at pH = 13.0

By looking for the difference between experimental data and simulated results, the percentages of total PFSA(start from n = 8, PFOA) and PFCS (start from n = 8, PFOS) to

form PFSA (n = 7, 6, 5, 4) and PFCS (n = 7, 6, 5, 4) were calculated by non-linear fitting model. From Figure 35, PFSA and PFCS degraded to non-detect percentages were 66.9% and 68.8% respectively. This process including two possible reaction pathways, one is that F atom was replaced by H atom, another way is removal of $-CF_2-$. Furthermore, the 31.6% of PFSA (n > 4) was removed the sulfonate headgroup with release of F^-. As for PFCA (n > 4), short chain products were formed from their parent compound. The ratio of above-mentioned process was 31.2% in PA-WATER sample.

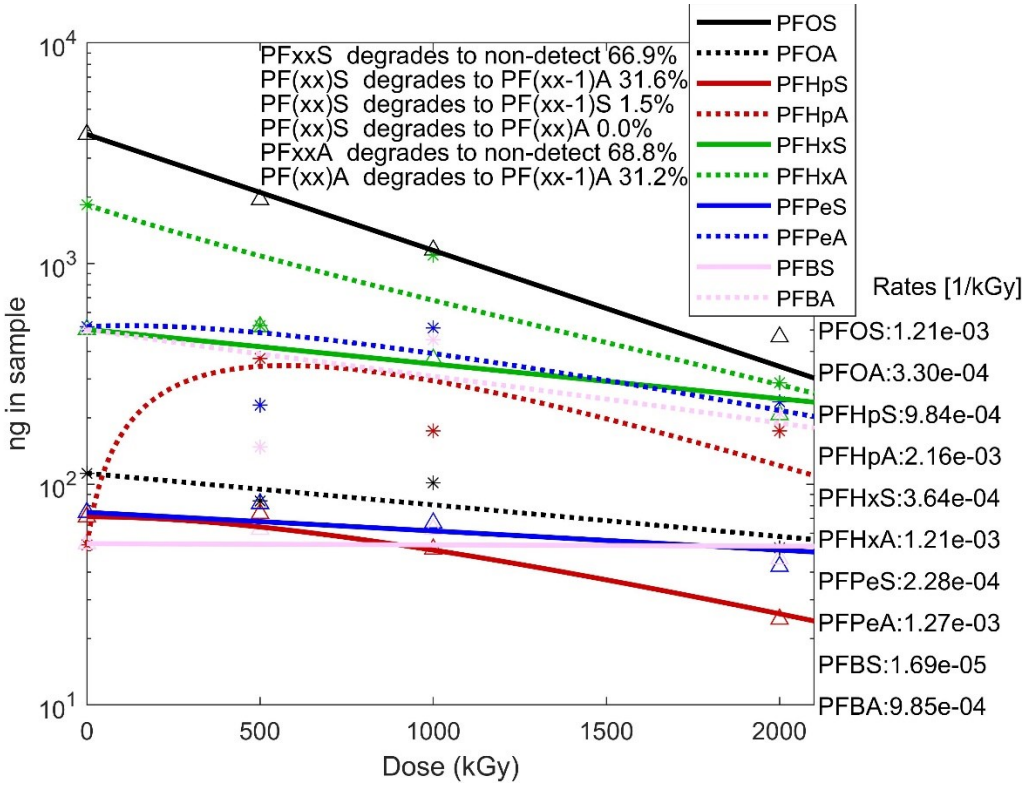

Figure 35: Degradation pathway of PA-WATER sample under different absorbed eBeam doses

It is demonstrated by figure 36 that 72.1% of the PFOS and partially fluorinated PFCAs reacted with hydrated electron and then formed fluoride ion. From the modeling results, the removal percentage of C-S bound is 25%.

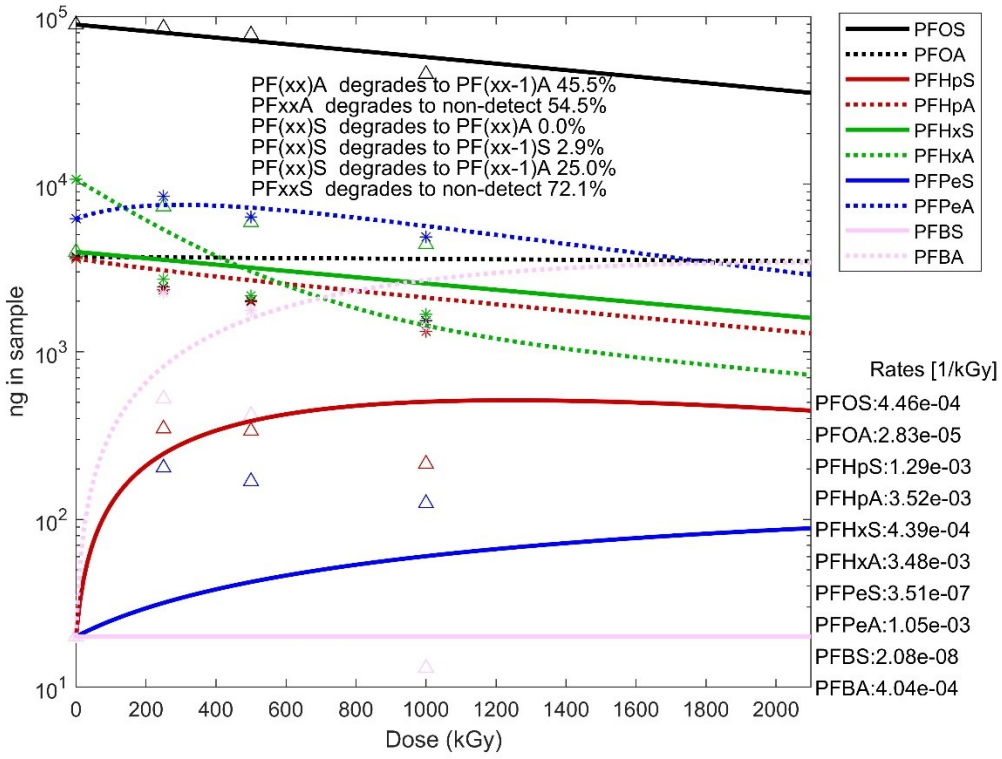

Figure 36: Mechanism of decomposition for MI-Soil sample

Rate constants for each compound were compared to investigate the effect of dose and other parameters. Figure 37 shows that PFOS and PFOA is much easier to compose in water rather than because we could see that the blue bar at PFOS is larger than the orange one. At the fielded sample and spiked sample, PFHpA rate constant is very high which means the breakdown of that specie is easier compared with other compounds. One more conclusion we could get that higher chain PFAS has better decomposed efficiency at water, soil matrix is good for lower chain degradation.

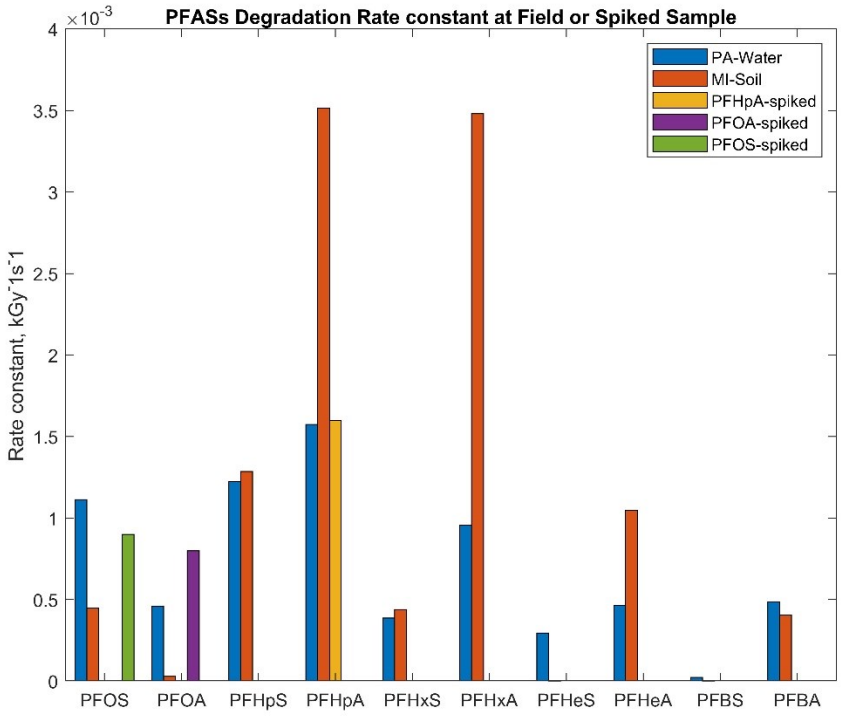

Figure 37: Degradation rate constant at felid or spiked sample

The main mechanism of degradation of PFOS by electron beam irradiation is as follows: the hydrated electrons and hydrogen radicals generated by the aqueous solution irradiated by electron beam have strong reducibility and can attack the fluorocarbon bond to make PFOS. The alkane sulfonic acid defluorinated, the free radical after removing one fluoride ion reacts with water and continues to repeat the reaction under the action of hydrated electrons and water molecules. The extremely unstable product obtained by the above reaction can spontaneously decompose to form short-chain PFOS and continue to defluorinated until mineralization.

CHAPTER V

CONCLUSIONS AND FUTURE PERSPECTIVES

This study applied of a high energy electron beam on the removal of PFASs in lab spiked sample, groundwater and soil. It was demonstrated the insight of PFAS decomposition by electron beam via analyzing the experimental and modeling results.

The low dose experiment results suggest that the efficiency of decompose PFOA/PFOS at 75 kGy is limited, then higher dose irradiation might be needed for fully removal of PFASs in water. For PFHpA, common water components (nitrate ion, bicarbonate, and fulvic acid) will not have negative effect on breakdown where the removal percentage at 75kGy is 100%. One important feature is higher pH had a positive effect on spiked PFHpA sample.

Despite these findings, effectiveness of eBeam removal PFAS in filed sample such as soil was performed. At 2000 kGy, PFOA and PFOS in soil matrix were almost fully removed, and the decomposition efficiencies were 98.8% and 98.6%, respectively. For Pennsylvania water sample, the breakdown percentage was about 88% at 2000 kGy. One point showed that eBeam technology is effective for the long chain PFAS and short chain PFAS at the same time.

From the kinetic model, spiked sample PFHpA was breakdown at pH 13 with rate constant of 0.0429 s^{-1}. This reaction is consistent with the pseudo first order kinetic model. In addition, PFOS in PA-WATER, MI-SOIL field sample was decomposed as rate of 1.21 x 10^{-3} $kGy^{-1}s^{-1}$, 4.46 x 10^{-4} $kGy^{-1}s^{-1}$ respectively. Therefore, PFOS in soil is more difficult to decompose in water might be due to other organic matters or concentration difference.

Further recommendations on expansion of current research can be presented as follows:

(1) evaluate and quantify the defluorination performance of PFHpA after electron beam irradiation.

(2) analyze all the immediate products from LC-MS untargeted results and propose a possible breakdown mechanism. Then, design experiment to prove and explain the pathway.

(3) apply eBeam to matrices such as surface water, wastewater, sediments, sludges, and landfill leachates.

(4) study the economy of eBeam technology on water or other matrix PFAS contaminated treatment.

REFERENCES

[1] A. B. Lindstrom, M. J. Strynar, and E. L. Libelo, "Polyfluorinated compounds: Past, present, and future," *Environ. Sci. Technol.*, vol. 45, no. 19, pp. 7954–7961, Oct. 2011.

[2] C. Lau, K. Anitole, C. Hodes, D. Lai, A. Pfahles-Hutchens, and J. Seed, "Perfluoroalkyl acids: A review of monitoring and toxicological findings," *Toxicol. Sci.*, vol. 99, no. 2, pp. 366–394, May 2007.

[3] M. Houde, A. O. De Silva, D. C. G. Muir, and R. J. Letcher, "Monitoring of perfluorinated compounds in aquatic biota: An updated review," *Environmental Science and Technology*, vol. 45, no. 19. pp. 7962–7973, 01-Oct-2011.

[4] M. Haukås, U. Berger, H. Hop, B. Gulliksen, and G. W. Gabrielsen, "Bioaccumulation of per- and polyfluorinated alkyl substances (PFAS) in selected species from the Barents Sea food web," *Environ. Pollut.*, vol. 148, no. 1, pp. 360–371, Jul. 2007.

[5] R. C. Buck *et al.*, "Perfluoroalkyl and polyfluoroalkyl substances in the environment: Terminology, classification, and origins," *Integr. Environ. Assess. Manag.*, vol. 7, no. 4, pp. 513–541, Oct. 2011.

[6] T. D. Appleman *et al.*, "Treatment of poly- and perfluoroalkyl substances in U.S. full-scale water treatment systems," *Water Res.*, vol. 51, pp. 246–255, Mar. 2014.

[7] I. Ross *et al.*, "A review of emerging technologies for remediation of PFASs," *Remediation*, vol. 28, no. 2, pp. 101–126, 2018.

[8] Y. Bao *et al.*, "Removal of perfluorooctane sulfonate (PFOS) and

perfluorooctanoate (PFOA) from water by coagulation: Mechanisms and influencing factors," *J. Colloid Interface Sci.*, vol. 434, pp. 59–64, 2014.

[9] E. Mariussen, "Neurotoxic effects of perfluoroalkylated compounds: Mechanisms of action and environmental relevance," *Arch. Toxicol.*, vol. 86, no. 9, pp. 1349–1367, 2012.

[10] V. A. Arias Espana, M. Mallavarapu, and R. Naidu, "Treatment technologies for aqueous perfluorooctanesulfonate (PFOS) and perfluorooctanoate (PFOA): A critical review with an emphasis on field testing," *Environ. Technol. Innov.*, vol. 4, pp. 168–181, 2015.

[11] V. M. Benitez, J. C. Yori, J. M. Grau, C. L. Pieck, and C. R. Vera, "Hydroisomerization and cracking of n-octane and n-hexadecane over zirconia catalysts," *Energy and Fuels*, vol. 20, no. 2, pp. 422–426, 2006.

[12] K. Prevedouros, I. T. Cousins, R. C. Buck, and S. H. Korzeniowski, "Sources, fate and transport of perfluorocarboxylates," *Environmental Science and Technology*, vol. 40, no. 1. pp. 32–44, 01-Jan-2006.

[13] Y. Gu, T. Liu, H. Wang, H. Han, and W. Dong, "Hydrated electron based decomposition of perfluorooctane sulfonate (PFOS) in the VUV/sulfite system," *Sci. Total Environ.*, vol. 607–608, pp. 541–548, 2017.

[14] J. S. Skaar, E. M. Ræder, J. L. Lyche, L. Ahrens, and R. Kallenborn, "Elucidation of contamination sources for poly- and perfluoroalkyl substances (PFASs) on Svalbard (Norwegian Arctic).," *Environ. Sci. Pollut. Res. Int.*, vol. 26, no. 8, pp. 7356–7363, Mar. 2019.

[15] A. K. Greaves and R. J. Letcher, “Linear and branched perfluorooctane sulfonate (PFOS) isomer patterns differ among several tissues and blood of polar bears,” *Chemosphere*, vol. 93, no. 3, pp. 574–580, 2013.

[16] K. Schulz, M. R. Silva, and R. Klaper, “Distribution and effects of branched versus linear isomers of PFOA, PFOS, and PFHxS: A review of recent literature,” *Sci. Total Environ.*, vol. 733, p. 139186, 2020.

[17] L. W. McKeen, “Producing fluoromonomers, fluoropolymers, and fluoropolymer finishing,” in *Fluorinated Coatings and Finishes Handbook*, Elsevier, 2016, pp. 13–50.

[18] S. E. Loveless *et al.*, “Comparative responses of rats and mice exposed to linear/branched, linear, or branched ammonium perfluorooctanoate (APFO),” *Toxicology*, vol. 220, no. 2, pp. 203–217, 2006.

[19] B. M. Sharma *et al.*, “Perfluoroalkyl substances (PFAS) in river and ground/drinking water of the Ganges River basin: Emissions and implications for human exposure,” *Environ. Pollut.*, vol. 208, pp. 704–713, 2016.

[20] Z. Lu *et al.*, “Occurrence and trends in concentrations of perfluoroalkyl substances (PFASs) in surface waters of eastern China,” *Chemosphere*, vol. 119, pp. 820–827, 2015.

[21] S. M. Bartell, A. M. Calafat, C. Lyu, K. Kato, P. B. Ryan, and K. Steenland, “Rate of decline in serum PFOA concentrations after granular activated carbon filtration at two public water systems in Ohio and West Virginia.,” *Environ. Health Perspect.*, vol. 118, no. 2, pp. 222–228, Feb. 2010.

[22] K. Hoffman, T. Webster, S. Bartell, M. Weisskopf, T. Fletcher, and V. Vieira, "Private drinking water wells as a source of exposure to perfluorooctanoic acid in communities surrounding a Washington, West Virginia fluoropolymer production facility," *Epidemiology*, vol. 22, no. 1, 2011.

[23] J. L. Domingo and M. Nadal, "Human exposure to per- and polyfluoroalkyl substances (PFAS) through drinking water: A review of the recent scientific literature," *Environ. Res.*, vol. 177, p. 108648, 2019.

[24] B. C. Crone *et al.*, "Occurrence of per- and polyfluoroalkyl substances (PFAS) in source water and their treatment in drinking water," *Crit. Rev. Environ. Sci. Technol.*, vol. 49, no. 24, pp. 2359–2396, Dec. 2019.

[25] A. Cordner, V. Y. De La Rosa, L. A. Schaider, R. A. Rudel, L. Richter, and P. Brown, "Guideline levels for PFOA and PFOS in drinking water: the role of scientific uncertainty, risk assessment decisions, and social factors," *J. Expo. Sci. Environ. Epidemiol.*, vol. 29, no. 2, pp. 157–171, 2019.

[26] C. P. Higgins and R. G. Luthy, "Sorption of perfluorinated surfactants on sediments," *Environ. Sci. Technol.*, vol. 40, no. 23, pp. 7251–7256, Dec. 2006.

[27] F. Xiao, M. F. Simcik, T. R. Halbach, and J. S. Gulliver, "Perfluorooctane sulfonate (PFOS) and perfluorooctanoate (PFOA) in soils and groundwater of a U.S. metropolitan area: Migration and implications for human exposure," *Water Res.*, vol. 72, pp. 64–74, 2015.

[28] Å. Høisæter, A. Pfaff, and G. D. Breedveld, "Leaching and transport of PFAS from aqueous film-forming foam (AFFF) in the unsaturated soil at a firefighting

training facility under cold climatic conditions," *J. Contam. Hydrol.*, vol. 222, no. September 2018, pp. 112–122, 2019.

[29] X. Lyu, X. Liu, Y. Sun, R. Ji, B. Gao, and J. Wu, "Transport and retention of perfluorooctanoic acid (PFOA)in natural soils: Importance of soil organic matter and mineral contents, and solution ionic strength," *J. Contam. Hydrol.*, vol. 225, no. April, p. 103477, 2019.

[30] M. L. Brusseau, R. H. Anderson, and B. Guo, "PFAS concentrations in soils: Background levels versus contaminated sites," *Sci. Total Environ.*, vol. 740, p. 140017, 2020.

[31] Y. Li *et al.*, "Half-lives of PFOS, PFHxS and PFOA after end of exposure to contaminated drinking water," *Occup. Environ. Med.*, vol. 75, no. 1, pp. 46–51, 2018.

[32] Q. Hu, J. N. Franklin, I. Bryan, E. Morris, A. Wood, and J. C. DeWitt, "Does developmental exposure to perfluorooctanoic acid (PFOA) induce immunopathologies commonly observed in neurodevelopmental disorders?," *Neurotoxicology*, vol. 33, no. 6, pp. 1491–1498, 2012.

[33] C. Briée, D. Moreira, and P. López-García, "Archaeal and bacterial community composition of sediment and plankton from a suboxic freshwater pond," *Res. Microbiol.*, vol. 158, no. 3, pp. 213–227, 2007.

[34] D. Zhang, W. Zhang, and Y. Liang, "Bacterial community in a freshwater pond responding to the presence of perfluorooctanoic acid (PFOA)," *Environ. Technol. (United Kingdom)*, 2019.

[35] R. Mahinroosta and L. Senevirathna, “A review of the emerging treatment technologies for PFAS contaminated soils,” *Journal of Environmental Management*, vol. 255. Academic Press, 01-Feb-2020.

[36] P. Li *et al.*, “Research progress on the removal of hazardous perfluorochemicals: A review,” *J. Environ. Manage.*, vol. 250, Nov. 2019.

[37] Z. Du *et al.*, “Adsorption behavior and mechanism of perfluorinated compounds on various adsorbents-A review,” *J. Hazard. Mater.*, vol. 274, pp. 443–454, 2014.

[38] M. Sörengård, E. Östblom, S. Köhler, and L. Ahrens, “Adsorption behavior of per- and polyfluoralkyl substances (PFASs) to 44 inorganic and organic sorbents and use of dyes as proxies for PFAS sorption,” *J. Environ. Chem. Eng.*, vol. 8, no. 3, p. 103744, 2020.

[39] S. Park, L. S. Lee, V. F. Medina, A. Zull, and S. Waisner, “Heat-activated persulfate oxidation of PFOA, 6:2 fluorotelomer sulfonate, and PFOS under conditions suitable for in-situ groundwater remediation,” *Chemosphere*, 2016.

[40] M. Inyang and E. R. V. Dickenson, “The use of carbon adsorbents for the removal of perfluoroalkyl acids from potable reuse systems,” *Chemosphere*, vol. 184, pp. 168–175, 2017.

[41] M. Ravichandran, G. R. Aiken, M. M. Reddy, and J. N. Ryan, “Enhanced dissolution of cinnabar (mercuric sulfide) by dissolved organic matter isolated from the Florida Everglades,” *Environ. Sci. Technol.*, vol. 32, no. 21, pp. 3305–3311, 1998.

[42] M. Saleem *et al.*, “Comparative performance assessment of plasma reactors for

the treatment of PFOA; reactor design, kinetics, mineralization and energy yield," *Chem. Eng. J.*, vol. 382, no. July 2019, p. 123031, 2020.

[43] P. Meng *et al.*, "Role of the air-water interface in removing perfluoroalkyl acids from drinking water by activated carbon treatment," *J. Hazard. Mater.*, vol. 386, no. December 2019, p. 121981, 2020.

[44] K. Yang and B. Xing, "Adsorption of organic compounds by carbon nanomaterials in aqueous phase: Polanyi theory and its application," *Chem. Rev.*, vol. 110, no. 10, pp. 5989–6008, 2010

[45] X. Xiao, B. A. Ulrich, B. Chen, and C. P. Higgins, "Sorption of poly- and perfluoroalkyl substances (PFASs) relevant to aqueous film-forming foam (AFFF)-impacted groundwater by biochars and activated carbon," *Environ. Sci. Technol.*, vol. 51, no. 11, pp. 6342–6351, 2017.

[46] X. Chen, X. Xia, X. Wang, J. Qiao, and H. Chen, "A comparative study on sorption of perfluorooctane sulfonate (PFOS) by chars, ash and carbon nanotubes," *Chemosphere*, vol. 83, no. 10, pp. 1313–1319, 2011.

[47] D. Q. Zhang, W. L. Zhang, and Y. N. Liang, "Adsorption of perfluoroalkyl and polyfluoroalkyl substances (PFASs) from aqueous solution - A review," *Science of the Total Environment*, vol. 694. Elsevier B.V., 01-Dec-2019.

[48] P. Chularueangaksorn, S. Tanaka, S. Fujii, and C. Kunacheva, "Adsorption of perfluorooctanoic acid (PFOA) onto anion exchange resin, non-ion exchange resin, and granular-activated carbon by batch and column," *Desalin. Water Treat.*, vol. 52, no. 34–36, pp. 6542–6548, Oct. 2014.

[49] L. W. Matzek and K. E. Carter, “Activated persulfate for organic chemical degradation: A review,” *Chemosphere*, vol. 151, pp. 178–188, 2016.

[50] H. Park, C. D. Vecitis, J. Cheng, N. F. Dalleska, B. T. Mader, and M. R. Hoffmann, “Reductive degradation of perfluoroalkyl compounds with aquated electrons generated from iodide photolysis at 254 nm,” *Photochem. Photobiol. Sci.*, vol. 10, no. 12, pp. 1945–1953, 2011.

[51] S. Yang *et al.*, “Degradation efficiencies of azo dye Acid Orange 7 by the interaction of heat, UV and anions with common oxidants: Persulfate, peroxymonosulfate and hydrogen peroxide,” *J. Hazard. Mater.*, vol. 179, no. 1, pp. 552–558, 2010.

[52] D. Zhao, X. Liao, X. Yan, S. G. Huling, T. Chai, and H. Tao, “Effect and mechanism of persulfate activated by different methods for PAHs removal in soil,” *J. Hazard. Mater.*, vol. 254–255, pp. 228–235, 2013.

[53] C. S. Liu, C. P. Higgins, F. Wang, and K. Shih, “Effect of temperature on oxidative transformation of perfluorooctanoic acid (PFOA) by persulfate activation in water,” *Sep. Purif. Technol.*, vol. 91, pp. 46–51, 2012.

[54] J. Cui, P. Gao, and Y. Deng, “Destruction of Per- A nd Polyfluoroalkyl Substances (PFAS) with Advanced Reduction Processes (ARPs): A Critical Review,” *Environmental Science and Technology*, vol. 54, no. 7. American Chemical Society, pp. 3752–3766, 07-Apr-2020.

[55] M. G. Antoniou, J. A. Shoemaker, A. A. De La Cruz, and D. D. Dionysiou, “Unveiling new degradation intermediates/pathways from the photocatalytic

degradation of microcystin-LR," *Environ. Sci. Technol.*, vol. 42, no. 23, pp. 8877–8883, 2008.

[56] J. CHEN, P. ZHANG, and J. LIU, "Photodegradation of perfluorooctanoic acid by 185 nm vacuum ultraviolet light," *J. Environ. Sci.*, vol. 19, no. 4, pp. 387–390, 2007.

[57] H. L. J. Bäckström, "The chain-reaction theory of negative catalysis," *J. Am. Chem. Soc.*, vol. 49, no. 6, pp. 1460–1472, 1927.

[58] Y. Bao *et al.*, "Degradation of PFOA substitute: GenX (HFPO-DA ammonium salt): oxidation with UV/Persulfate or reduction with UV/Sulfite?," *Environ. Sci. Technol.*, vol. 52, no. 20, pp. 11728–11734, 2018.

[59] J. Wang and S. Wang, "Activation of persulfate (PS) and peroxymonosulfate (PMS) and application for the degradation of emerging contaminants," *Chem. Eng. J.*, vol. 334, pp. 1502–1517, 2018.

[60] D. Liu *et al.*, "Perfluorooctanoic acid degradation in the presence of Fe(III) under natural sunlight," *J. Hazard. Mater.*, vol. 262, pp. 456–463, 2013.

[61] H. Tang, Q. Xiang, M. Lei, J. Yan, L. Zhu, and J. Zou, "Efficient degradation of perfluorooctanoic acid by UV–Fenton process," *Chem. Eng. J.*, vol. 184, pp. 156–162, 2012.

[62] F. Hao, W. Guo, A. Wang, Y. Leng, and H. Li, "Intensification of sonochemical degradation of ammonium perfluorooctanoate by persulfate oxidant," *Ultrason. Sonochem.*, vol. 21, no. 2, pp. 554–558, 2014.

[63] K. H. Kucharzyk, R. Darlington, M. Benotti, R. Deeb, and E. Hawley, "Novel

treatment technologies for PFAS compounds: A critical review," *J. Environ. Manage.*, vol. 204, pp. 757–764, 2017.

[64] C. D. Vecitis, Y. Wang, J. Cheng, H. Park, B. T. Mader, and M. R. Hoffmann, "Sonochemical degradation of perfluorooctanesulfonate in aqueous film-forming foams," *Environ. Sci. Technol.*, vol. 44, no. 1, pp. 432–438, 2010.

[65] L. Rodriguez-Freire *et al.*, "Sonochemical degradation of perfluorinated chemicals in aqueous film-forming foams," *J. Hazard. Mater.*, vol. 317, pp. 275–283, 2016.

[66] J.-C. Lin, S.-L. Lo, C.-Y. Hu, Y.-C. Lee, and J. Kuo, "Enhanced sonochemical degradation of perfluorooctanoic acid by sulfate ions," *Ultrason. Sonochem.*, vol. 22, pp. 542–547, 2015.

[67] M. Trojanowicz, A. Bojanowska-Czajka, I. Bartosiewicz, and K. Kulisa, "Advanced oxidation/reduction processes treatment for aqueous perfluorooctanoate (PFOA) and perfluorooctanesulfonate (PFOS) – A review of recent advances," *Chemical Engineering Journal*, vol. 336. Elsevier B.V., pp. 170–199, 15-Mar-2018.

[68] L. Jin, P. Zhang, T. Shao, and S. Zhao, "Ferric ion mediated photodecomposition of aqueous perfluorooctane sulfonate (PFOS) under UV irradiation and its mechanism," *J. Hazard. Mater.*, vol. 271, pp. 9–15, 2014.

[69] Y. Qu, C. Zhang, F. Li, J. Chen, and Q. Zhou, "Photo-reductive defluorination of perfluorooctanoic acid in water," *Water Res.*, vol. 44, no. 9, pp. 2939–2947, 2010.

[70] J. Cui, P. Gao, and Y. Deng, "Destruction of per- and polyfluoroalkyl substances

(PFAS) with advanced reduction processes (ARPs): a critical review," *Environ. Sci. Technol.*, vol. 54, no. 7, pp. 3752–3766, 2020.

[71] S.-H. Ma *et al.*, "EB degradation of perfluorooctanoic acid and perfluorooctane sulfonate in aqueous solution," *Nucl. Sci. Tech.*, vol. 28, no. 9, p. 137, 2017.

[72] S. Park, L. S. Lee, V. F. Medina, A. Zull, and S. Waisner, "Heat-activated persulfate oxidation of PFOA, 6:2 fluorotelomer sulfonate, and PFOS under conditions suitable for in-situ groundwater remediation," *Chemosphere*, vol. 145, pp. 376–383, 2016.

[73] M. Fischer and P. Warneck, "Photodecomposition and photooxidation of hydrogen sulfite in aqueous solution," *J. Phys. Chem.*, vol. 100, no. 37, pp. 15111–15117, 1996.

[74] Y. Gu, T. Liu, H. Wang, H. Han, and W. Dong, "Hydrated electron based decomposition of perfluorooctane sulfonate (PFOS) in the VUV/sulfite system," *Sci. Total Environ.*, vol. 607–608, pp. 541–548, 2017.

[75] M. M. J. Oosthuizen and D. Greyling, "Hydroxyl radical generation: The effect of bicarbonate, dioxygen and buffer concentration on pH-dependent chemiluminescence," *Redox Rep.*, vol. 6, no. 2, pp. 105–116, 2001.

[76] R. Chen and G. R. Freeman, "Solvent effects on reactivity of solvated electrons with nitrate ion and on electrolyte conductivity in C1 to C10 n-alcohols," *J. Phys. Chem.*, vol. 99, no. 14, pp. 4970–4975, 1995.

[77] J. A. Leenheer and J.-P. Croué, "Peer reviewed: characterizing aquatic dissolved organic matter," *Environ. Sci. Technol.*, vol. 37, no. 1, pp. 18A-26A, 2003.

[78] J. N. Uwayezu, L. W. Y. Yeung, and M. Bäckström, “Sorption of PFOS isomers on goethite as a function of pH, dissolved organic matter (humic and fulvic acid) and sulfate,” *Chemosphere*, vol. 233, pp. 896–904, 2019.

[79] A. Y. C. Lin, S. C. Panchangam, C. Y. Chang, P. K. A. Hong, and H. F. Hsueh, “Removal of perfluorooctanoic acid and perfluorooctane sulfonate via ozonation under alkaline condition,” *J. Hazard. Mater.*, vol. 243, pp. 272–277, 2012.

[80] Rodi, R. M. “Preliminary results of perfluorooctanesulfonic acid removal via electron beam at various doses, ” *Master’s thesis, Texas A&M University.,* vol.53, pp.1689-1699, 2019.

APPENDIX

MATLAB code to solve kinetic function was attached here.

```
function DY = ODEFUN_PFAS(T,Y,params)
% this function solves a set of differential equation for
the degradation
% of species as a function of time

DR = 17.19; % 10 kGy/s ebeam dose rate is fixed at 10

r8_ND = params(1); % fraction of PFxxS  which goes to non-
detect
Coef2 = params(2); % remaining fract CS remove S
Coef3 = params(3); % remaining fract CS remove C
b(1) = params(4); % PFOS overall rate
b(2) = params(5); %PFOA overall rate
r8a_ND = params(6); % fraction of PFxxA which goes to non-
detect
b(3) = params(7);% PFHpS overall rate
b(4) = params(8);% PFHpA overall rate
b(5) = params(9);% PFHxS overall rate
b(6) = params(10);% PFHxA overall rate
b(7) = params(11);% PFPeS overall rate
b(8) = params(12);% PFPeA overall rate
b(9) = params(13);% PFBS overall rate
b(10) = params(14);% PFBA overall rate


r8_ND = r8_ND; %fract remove to non-detect
r8_S = Coef2*(1-r8_ND);% fract remove S
r8_C = Coef3*(1-r8_ND); % fract remove C
r8_CS = 1-r8_ND-r8_S-r8_C ; % fract remove CS
r8a_ND = r8a_ND; %fract remove to non-detect
r8a_C = 1-r8a_ND; % fract remove C

r7_ND = r8_ND; %remove to non-detect
r7_S = Coef2*(1-r7_ND);% remove S
r7_C = Coef3*(1-r7_ND); % remove C
r7_CS = 1-r7_ND-r7_S-r7_C ; % remove CS
r7a_ND = r8a_ND; %remove to non-detect
r7a_C = 1-r7a_ND; % remove C
```

```
r6_ND = r8_ND; %fract remove to non-detect
r6_S = Coef2*(1-r6_ND);% fract remove S
r6_C = Coef3*(1-r6_ND); % fract remove C
r6_CS = 1-r6_ND-r6_S-r6_C ; % fract remove CS
r6a_ND = r8a_ND; %fract remove to non-detect
r6a_C = 1-r6a_ND; % fract remove C

r5_ND = r8_ND; %fract remove to non-detect
r5_S = Coef2*(1-r5_ND);% fract remove S
r5_C = Coef3*(1-r5_ND); % fract remove C
r5_CS = 1-r5_ND-r5_S-r5_C ; % fract remove CS
r5a_ND = r8a_ND; %fract remove to non-detect
r5a_C = 1-r5a_ND; % fract remove C

r4_ND = r8_ND; %fract remove to non-detect
r4_S = Coef2*(1-r4_ND);% fract remove S
r4_C = Coef3*(1-r4_ND); % fract remove C
r4_CS = 1-r4_ND-r4_S-r4_C ; % fract remove CS
r4a_ND = r8a_ND; %fract remove to non-detect
r4a_C = 1-r4a_ND; % fract remove C


N_PFOS=Y(1);
N_PFOA=Y(2);
N_PFHpS=Y(3);
N_PFHpA=Y(4);
N_PFHxS=Y(5);
N_PFHxA=Y(6);
N_PFPeS=Y(7);
N_PFPeA=Y(8);
N_PFBS=Y(9);
N_PFBA=Y(10);
Dose = Y(11);
Temp = Y(12);

DN_PFOS= - b(1)*DR*N_PFOS;
DN_PFOA= - b(2)*DR*N_PFOA + r8_S*b(1)*DR*N_PFOS;
DN_PFHpS= - b(3)*DR*N_PFHpS + r8_C*b(1)*DR*N_PFOS;
DN_PFHpA=- b(4)*DR*N_PFHpA + r8_CS*b(1)*DR*N_PFOS +
r8a_C*b(2)*DR*N_PFOA + r7_S*b(3)*DR*N_PFHpS;
DN_PFHxS=- b(5)*DR*N_PFHxS + r7_C*b(3)*DR*N_PFHpS;
DN_PFHxA=- b(6)*DR*N_PFHxA + r6_S*b(5)*DR*N_PFHxS +
r7a_C*b(4)*DR*N_PFHpA + r7_CS*b(3)*DR*N_PFHpS;
DN_PFPeS=- b(7)*DR*N_PFPeS + r6_C*b(5)*DR*N_PFHxS;
```

```
DN_PFPeA=- b(8)*DR*N_PFPeA + r6_CS*b(5)*DR*N_PFHxS +
r6a_C*b(6)*DR*N_PFHxA+ r5_S*b(7)*DR*N_PFPeS;
DN_PFBS= -b(9)*DR*N_PFBS + r5_C*b(7)*DR*N_PFPeS;
DN_PFBA=- b(10)*DR*N_PFBA + r4_S*b(9)*DR*N_PFBS +
r5a_C*b(8)*DR*N_PFPeA +r5_CS*b(7)*DR*N_PFPeS;
DDose = DR;
specheat = 1.5; % kJ/kg-C
Tinf = 25;
hA = 33*0.4; % w/C assumes h W/m^2-K and 0.4 m^2
DTemp = DR/specheat - hA*(Temp-Tinf)/1e3;
%DN_C = r8_C*b(1)*DR*N_PFOS + b(2)*DR*N_PFOA
%DN_S = r8_S*b(1)*DR*N_PFOS + r7_S*b(3)*DR*N_PFHpS
%DN_CS = r8_CS*b(1)*DR*N_PFOS
DY =
[DN_PFOS;DN_PFOA;DN_PFHpS;DN_PFHpA;DN_PFHxS;DN_PFHxA;DN_PFP
eS;DN_PFPeA;DN_PFBS;DN_PFBA;DDose;DTemp];
```

Best Fit Model data processing

```
function diff=findPFASdiff(dose,Conc,Doses,ng_D)
% compare given experimental and model data
for i =1:length(Doses)
    modconc = interp1(dose,Conc,Doses(i));
    expconc = ng_D(i,:);
    dif(i,:) = modconc-expconc;
    logdif(i,:) = log(modconc)-log(expconc);
end
dif
size(sum(dif.^2))
%save logdif.mat logdif
diff2 = (sqrt(sum(sum(dif.^2))))/max(max(expconc)); % least
squares in linear space
diff3 = (sqrt(sum(sum(logdif.^2))))/log(max(max(expconc)));
% least squares in log space
diff = 0.99*diff2+0.01*diff3;
[diff2,diff3,diff]
End
```

Best Fit Model data processing

```
clear
clc
close all

guessparams = 1e-2*[75    5    5    0.1215    0.0352   85
0.1027    0.1722    0.0373    0.1080    0.0224    0.0738
0.0000    0.0590];

Names =
{'PFOS','PFOA','PFHpS','PFHpA','PFHxS','PFHxA','PFPeS','PFP
eA','PFBS','PFBA'};
para_inds = [4,5,7,8,9,10,11,12,13,14];

%params(1); % fraction of PFxxS  which goes to non-detect
%params(2); % remaining fract CS remove S
%params(3); % remaining fract CS remove C
%params(4); % PFOS overall rate
%params(5); %PFOA overall rate
%params(6); % fraction of PFxxA which goes to non-detect
%params(7);% PFHpS overall rate
%params(8);% PFHpA overall rate
%params(9);% PFHxS overall rate
%params(10);% PFHxA overall rate
%params(11);% PFPeS overall rate
%params(12);% PFPeA overall rate
%params(13);% PFBS overall rate
%params(14);% PFBA overall rate
options = optimset('fminsearch');
options.TolFun = 1e-4;
options.TolX = 1e-6;

params =
fminsearch(@FunctionalModelPFAS,guessparams,options);


exp_header = {'Dose kGy' 'mL initial'   'mL post treatment'
     'PFBA'    'PFPEA-1' 'PFHXA-1' 'PFHPA-1' 'PFOA-1'
     'PFBS-1'  'PFPES-1' 'PFHXS-1' 'PFHPS-1' 'PFOS-1'};
exp_dat = [
0    50   50   0    0    0    39224.33333    0
     1169.861093    0    0    0    0
5    50   50   0    42.14237397    0    6809.666667    0
     895.4202053    0    0    0    0
10   50   50   0    53.86776056    0    3660.666667    0
     1104.459502    0    0    0    0
```

```
25   50   50   0    0    0    21.66666667    0
     933.5485654    0    0    0    0
50   50   50   0    0    0    0    0    1185.245698    0
     0    0    0
75   50   50   0    0    0    0    0    1064.804117    0
     0    0    0]; % ng/L

save expdata.mat exp_header exp_dat



ng_D(1,:) =
(exp_dat(1,3)/1000)*exp_dat(1,[13,8,12,7,11,6,10,5,9,4]);
ng_D(2,:) =
(exp_dat(2,3)/1000)*exp_dat(2,[13,8,12,7,11,6,10,5,9,4]);
ng_D(3,:) =
(exp_dat(3,3)/1000)*exp_dat(3,[13,8,12,7,11,6,10,5,9,4]);
ng_D(4,:) =
(exp_dat(4,3)/1000)*exp_dat(4,[13,8,12,7,11,6,10,5,9,4]);
Doses = exp_dat(1:4,1);

f1 = figure;
p1=plot(Doses,ng_D,'^');
cols = jet(length(p1))*0.8;
cols = [0,0,0
    0,0,0
    0.8,0,0
    0.8,0,0
    0,0.7,0
    0,0.7,0
    0,0,1
    0,0,1
    1,0.8,1
    1,0.8,1
    ];
for i=1:length(p1)
    set(p1(i),'color',cols(i,:))
    if i == round(i/2)*2;
        set(p1(i),'marker','*')
    end
    set(p1(i),'HandleVisibility','off')
end

initconc = [ng_D(1,:),0,25];
time = linspace(0,215,201);
```

```
[tout,yout] =
ode45(@(t,y)ODEFUN_PFAS(t,y,params),time,initconc);

dose = yout(:,11);
Conc = yout(:,1:10);
Temp = yout(:,12);

f2 = figure;
plot(time,Temp)


diff = findPFASdiff(dose,Conc,Doses,ng_D);

figure(f1)
hold on
p1=plot(dose,Conc);
for i=1:length(p1)
    set(p1(i),'color',cols(i,:))
    set(p1(i),'linewidth',2)
    if i == round(i/2)*2;
        set(p1(i),'linestyle',':')
    end

end
hold off
% p2 =plot(dose,sum(Conc,2),'k');
% set(p2,'linewidth',2)
 l1 = legend(Names)
 xlim([0,75])
set(gca,'yscale','log')
set(gca,'position',[0.1,0.1,0.7,0.85])
set(l1,'position',[0.71,0.8,0.1,0])
xlabel('Dose (kGy)')
ylabel('ng in sample')

DR = 10; %kJ/kg/s
text(max(xlim)*1.08,8e2,'Rates [1/kGy]')
aa = logspace(2.7,0.5,10);
for i=1:length(aa)

text(max(xlim)*1.005,aa(i),[Names{i},':',num2str(params(par
a_inds(i)),'%.2e')])
end
```

```
aa = 1.2*logspace(3.5,2,5);
text(50,aa(1),['PFxxS  degrades to non-detect
',num2str(params(1)*100,'%2.1f'),'%'])
text(50,aa(2),['PF(xx)S  degrades to PF(xx-1)A
',num2str((1-params(1))*(1-params(2)-
params(3))*100,'%2.1f'),'%'])
text(50,aa(3),['PF(xx)S  degrades to PF(xx-1)S
',num2str((1-params(1))*params(3)*100,'%2.1f'),'%'])
text(50,aa(4),['PF(xx)S  degrades to PF(xx)A ',num2str((1-
params(1))*params(2)*100,'%2.1f'),'%'])
text(50,aa(5),['PFxxA  degrades to non-detect
',num2str(params(6)*100,'%2.1f'),'%'])
text(50,aa(6),['PF(xx)A  degrades to PF(xx-1)A
',num2str((1-params(6))*100,'%2.1f'),'%'])

print('PFAS_FitResults.jpg','-djpeg','-r600')



clear
clc
close all

Dose = [0,500,1000,2000]; % kJ/kg
PFOS = [1450.5,631.3,344.1,163.4]; % ng
samplesize = 100; %[mL]
sampledensity = 1e-3; %[kg/mL]
PFOS_C = PFOS/samplesize;
inputenergy_kJ = Dose*sampledensity*samplesize; %[kJ]
e = 1.602e-19; %[J/eV]
inputenergy_eV = inputenergy_kJ/1000/e; % [eV]
WaterAMU = 18; %[g/mole];
NA = 6.022e23; %[molecule/mole]
SEI_eV = Dose*1000/1000*WaterAMU/e/NA; %[eV/molecule]


NLM = fitnlm(Dose,PFOS_C,'P ~ b0*exp(-b1*D)',[PFOS(1),0]);
xfit = linspace(min(Dose),max(Dose),100);
yfit = predict(NLM,xfit');
expr = NLM.Formula.Expression;
expr = strrep(expr,'^','\^');
Coef = table2array(NLM.Coefficients);
b0 = Coef(1,1);
b1 = Coef(2,1);
```

```
p1=plot(Dose,PFOS_C,'o-',xfit,yfit,':');
set(p1(2),'linewidth',2)
L1=legend('Experiment',['Non-Linear Regression Model:
',NLM.Formula.ResponseName,' = ',expr]);
text(xfit(30),yfit(10),['Adjusted
R^2=',num2str(NLM.Rsquared.Adjusted)])
text(xfit(30),yfit(15),['b0=',num2str(b0),', pval =
',num2str(Coef(1,4))])
text(xfit(30),yfit(20),['b1=',num2str(b1),', pval =
',num2str(Coef(2,4))])
set(gca,'fontsize',12)
xlabel('Dose (kGy)')
ylabel('PFOS (ng/mL)')
title('100 mL michigan field water sample')


     Amount of LC-MS targeted degradation compounds
clear
clc
close all

a=importdata('DataForFinalReports(3).xlsx');
b = a.data.Final0x28ND0x3D00x29;
c = a.textdata.Final0x28ND0x3D00x29;

CompLabels = {c{15:43,1}};
Samp = {c{2,2:11}};
ST = {c{4,2:11}};

Dose = b(1,:);
OMass = b(3,:);
FMass = b(4,:);
CMass = b(5,:);
C2Mass = OMass-FMass;
CUnR = C2Mass -  CMass;

Conc = b(13:41,:);

for ii = 1:length(Samp)
    ngMass(:,ii) = Conc(:,ii)*FMass(ii);
    %if ST{ii}=='W'
        ngConc(:,ii) = Conc(:,ii);
    % else
```

```
    % ngConc(:,ii) = Conc(:,ii)*FMass(ii)/OMass(ii);
        % water samples need to be corrected for change in
volume6
    %end

end

ngConc(isnan(ngConc)) = 0;

Dose
SoilInd = find(strcmp(ST,'S'));
SoilInd = [4,1,2,3,9]
ngConc(:,9) = ngConc(:,9)/1e3; %correct ng/L to ng/g
NDValue = 0.5;
%ngConc = ngConc+NDValue;

WaterInd = find(strcmp(ST,'W'));
WaterInd = [10,5,6,7,8]

CompLabels
CV = 1:length(CompLabels)

f1 = figure
set(gcf,'position',[100,100,1700,700])
bar(CV,ngConc(:,SoilInd))
set(gca,'fontsize',14)
ylabel('ng/g-dry')
set(gca,'xtick',CV)
set(gca,'xticklabel',CompLabels)
set(gca,'XTickLabelRotation',90)
title('Michigan IDW Soil')
legend(Samp(SoilInd))
colormap(jet)
ylim([0,1000])
a1 = gca;

f2 = figure;
a2 = copyobj(a1,f2);
set(gcf,'position',[120,120,1700,700])
colormap(jet)
legend(Samp(SoilInd))
ylim([0,100])

f3 = figure
set(gcf,'position',[140,140,1700,700])
```

```
bar(CV,ngMass(:,WaterInd))
set(gca,'fontsize',14)
ylabel({'100 mL sample','Remaining component ammount
(ng)'})
set(gca,'xtick',CV)
set(gca,'xticklabel',CompLabels)
set(gca,'XTickLabelRotation',90)
title('Pennsylvania IDW Water')
legend(Samp(WaterInd))
colormap(jet)
ylim([0,5e6])
a3 = gca;
title('Water IDW Component Concentrations')
print(gcf,['WaterIDW','_Component Concentration.png'],'-
dpng','-r900')


f4 = figure;
a4 = copyobj(a3,f4);
set(gcf,'position',[160,160,1700,700])
colormap(jet)
legend(Samp(WaterInd))
ylim([0,5e5])
title('Water IDW Component Concentrations')
print(gcf,['WaterIDW','_Component
Concentration_Zoom.png'],'-dpng','-r900')


f5 = figure

WaterInd = [10,5,6,7]
majorComp = max(ngMass,[],2)>1e5
p1 = plot(Dose(WaterInd),ngMass(majorComp,WaterInd),'-')
markers = {'x','o','d','<','>','*','^'}
for ii = 1:7
    set(p1(ii),'marker',markers{ii})
    set(p1(ii),'linewidth',2)
end
L1=legend(CompLabels(majorComp))
set(gca,'fontsize',14)

xlabel('Dose (kGy)')
ylabel({'100 mL sample','Remaining component ammount
(ng)'})
set(gca,'yscale','log')
```

```
title('Component Kinetics')
set(L1,'position',[0.75,0.64,0.17,0.35])
print(gcf,['WaterIDW','_Component Kinetics.png'],'-dpng','-
r900')
```